Article:

Spychala, YT, Hodgson, DM orcid.org/0000-0003-3711-635X and Lee, DR orcid.org/0000-0003-4397-6030 (2017) Autogenic controls on hybrid bed distribution in submarine lobe complexes. Marine and Petroleum Geology, 88. pp. 1078-1093. ISSN 0264-8172

https://doi.org/10.1016/j.marpetgeo.2017.09.005

Accepted Manuscript

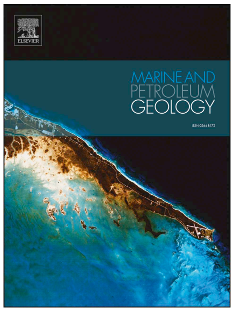

Autogenic controls on hybrid bed distribution in submarine lobe complexes

Y.T. Spychala, D.M. Hodgson, D.R. Lee

PII: S0264-8172(17)30352-5

DOI: 10.1016/j.marpetgeo.2017.09.005

Reference: JMPG 3063

To appear in: *Marine and Petroleum Geology*

Received Date: 23 May 2017

Revised Date: 28 August 2017

Accepted Date: 4 September 2017

Please cite this article as: Spychala, Y.T., Hodgson, D.M., Lee, D.R., Autogenic controls on hybrid bed distribution in submarine lobe complexes, *Marine and Petroleum Geology* (2017), doi: 10.1016/j.marpetgeo.2017.09.005.

Autogenic controls on hybrid bed distribution in submarine lobe complexes

Spychala, Y.T[1†*], Hodgson, D.M.[1], Lee, D.R.[1]

[1]Stratigraphy Group, School of Earth and Environment, University of Leeds, LS2 9JT Leeds, UK

[†]now at: Department of Earth Science, University of Utrecht, 3584 CS Utrecht, NL

*corresponding author: y.t.spychala@uu.nl

Abstract

Hybrid beds, the deposits of sediment gravity flows that show evidence for more than one flow regime (turbulent, transitional and/or laminar), have been recognized as important components of submarine lobe deposits. A wide range of hybrid bed types have been documented, however, quantitative analysis of the stratigraphic and geographic distribution of these enigmatic bed types is rare. Here, extensive exposures integrated with research borehole data from Unit A of the Laingsburg Formation and Fan 4 of the Skoorsteenberg Formation, Ecca Group, South Africa, provide the opportunity to examine geographical and stratigraphic patterns over a range of hierarchical scales.

For this purpose, >23,000 individual beds have been evaluated for deposit type and bed thickness. On average, hybrid beds make up < 5% of all events and < 10% of the cumulative thickness. Lobe complex 1 (LC1) of Fan 4 ,Skoorsteenberg Formation, preserves a prominent geographical trend of hybrid beds becoming more prevalent towards the frontal fringes of a lobe complex (up to 33.2% of beds), whereas their proportion in proximal and medial lobe complex settings is < 10%.

Data from Unit A, Laingsburg Formation, show hybrid beds are less common in the basal (A.1) and top (A.6) subunits compared to A.2-A.5 in both core data sets. The bases and tops of some lobe complexes (A.2, A.3 and A.5.7) are observed to be slightly enriched in hybrid beds, whereas others (A.5.1, A.5.5 and A.6.1) show no hybrid beds in their bases, which does not conform to expected allogenically-driven distributions that predict more hybrid beds during the initiation of lobe complexes. Instead, the occurrence and distribution of hybrid beds in lobe complexes are interpreted to be controlled by autogenic processes, including flow transformation processes on the basin-floor meaning enrichment in frontal lobe fringe settings. Therefore, the 1D distribution of hybrid beds in lobe complexes reflects the dominant stacking pattern of lobes within a lobe complex, with enrichment at the base and top of lobe complexes due to overall progradational to retrogradational stacking patterns. Individual lobes show a wide range of hybrid bed distributions, due to stacking patterns of the component lobe elements. These findings highlight the importance of autogenic processes rather than allogenic controls in the distribution of hybrid beds, which has implications for reservoir evaluation and the assessment of lobe stacking patterns in 1D core data sets.

Keywords: hybrid beds, distribution trends, autogenic controls, allogenic controls, lobes, deepwater fans

1. Introduction

Basin-floor lobes generally comprise three deposit types: turbidites, hybrid beds and debrites (Talling et al., 2004; Hodgson, 2009; Etienne et al., 2012). Hybrid beds comprise a division that was deposited by a turbulent flow and a division that was deposited by a debritic flow and have been recognized as an important part of the rock record in lobe deposits (e.g. Haughton et al. 2003; Ito, 2008; Hodgson, 2009; Talling et al., 2012a; Etienne et al., 2012;

Grundvåg et al., 2014; Patacci et al., 2014; Collins et al., 2015; Fonnesu et al., 2015, 2017). Understanding controls on the geographic and stratigraphic distribution of hybrid event beds is important as these introduce bed-scale reservoir heterogeneities due to vertical superposition of reservoir and non-reservoir lithologies (Amy et al. 2009; Davis et al., 2009; Haughton et al., 2009, Porten et al., 2016). Core and outcrop data sets have enabled several hybrid bed classifications to be established (e.g. Haughton et al., 2003; Talling et al., 2004; Ito, 2008; Davis et al., 2009; Haughton et al., 2009; Hodgson, 2009; Jackson et al., 2009; Magalhaes and Tinterri, 2010; Kane & Pontén, 2012; Patacci et al., 2014; Fonnesu et al., 2015, 2017; Southern et al., 2017; Pierce et al., in review). In addition, laboratory experiments have been conducted to study how flow processes control hybrid bed deposition (Baas et al., 2009; Sumner et al., 2009; Baas et al., 2011).

Several studies have indicated that hybrid beds are more prevalent in the distal parts of submarine fan and lobe settings (Talling et al., 2004; Ito, 2008; Hodgson, 2009; Pyles & Jennette, 2009; Talling et al., 2012a; Etienne et al., 2012; Kane and Pontén, 2012; Grundvåg et al., 2014; Collins et al., 2015; Fonnesu et al., 2015; 2016; Southern et al., 2017; Pierce et al., review). Where hybrid beds have been observed in more proximal lobe settings (Ito, 2008; Jackson et al., 2009; Terlaky et al., 2016; Fonnesu et al., 2017) enhanced erosion and deceleration have been invoked due to processes occurring in the channel-lobe transition zone and basin confinement. Their stratigraphic distribution has been linked to the character of the supply slope and seabed relief, where hybrid beds are invoked to develop during periods of disequilibrium over steep, out-of-grade slopes (Haughton et al., 2003; 2009; Hodgson, 2009; Pierce et al., in review), and therefore are dominantly deposited during fan initiation and growth phases, or initiated by flow expansion in the channel-lobe transition zone (Ito, 2008; Kane and Pontén, 2012). Quantitative analysis on the predictability of geographic and stratigraphic distribution of these deposits has seldom been attempted. Davis et al. (2009) presented statistical analysis on hybrid beds from the outer Forties Fan, Central North Sea. They assessed >1000 event beds, of which 67% were hybrid beds, and 81% in terms of bed thickness. However, this analysis incorporated data from different field areas, and correlation between the fields was hindered by field-specific fossil assemblages. Recently, Pierce et al. (in review) reviewed the hybrid bed distribution in the Ross Sandstone Formation, Clare Basin, Ireland. They showed that overall the proportion of hybrid beds decreases from the lower, through mid to upper Ross Formation (89%, 21% and 14% in thickness). Vertical trends are interpreted to reflect either progradation of proximal over distal parts of the system (Collinson et al., 1991; Wignall and Best, 2000) or out-of-equilibrium slopes that led to enhanced erosion (Haughton et al., 2009). Fonnesu et al. (2017) documented hybrid beds across several sub-environments from the North Apennine Gottero Sandstone, NW-Italy and interpreted their stratigraphic distribution to reflect lobe stacking patterns. However, in these studies the internal architecture and different stratigraphic scales of the deposited submarine fan (lobe hierarchy) are not discussed.

Here, we present a multi-scale quantitative analysis of geographic and stratigraphic hybrid bed distributions from an outcrop and core data set from the palaeogeographically well-constrained Fan 4 (Skoorsteenberg Formation, Tanqua depocentre) and Unit A (Laingsburg Formation, Laingsburg depocentre) systems of the Karoo Basin, South Africa. Specific objectives are to: 1) establish proximal to distal trends of hybrid beds within a lobe complex; 2) examine stratigraphic trends at lobe complex set, lobe complex and lobe scales; 3) discuss the factors that control the observed trends; and 4) discuss the implication of hybrid bed distribution on recognising stacking patterns from 1D data sets.

2. Geological Setting

Traditionally, the Karoo Basin is interpreted as a retroarc foreland basin connected to a magmatic arc and fold-thrust belt (Visser and Prackelt, 1996; Visser, 1997; Catuneanu et al., 1998). More recently, Tankard et al. (2009) suggested that subsidence during the early deep-water phase of deposition pre-dates the effects of loading by the Cape Fold Belt and was induced by dynamic topography associated with mantle flow processes coupled with distant subduction of the palaeo-Pacific plate (Pysklywec and Mitrovica, 1999). This study focusses on deposits of the Ecca Group (Wickens, 1994; Flint et al., 2011) deposited during an early deep-water phase in the Tanqua and Laingsburg depocentres of the southwest Karoo Basin (Fig. 1a). In both areas, the Ecca Group represents an overall shallowing-upward succession of sediments from deep-water to fluvial settings (Flint et al., 2011).

2.1 Tanqua depocentre

The Tanqua depocentre is located in the southwest of the Karoo Basin (Fig. 1a, b). This study focuses on deposits of Fan 4 of the Skoorsteenberg Formation (Fig. 2), one of four sand-prone basin-floor channel-lobe systems (Bouma and Wickens, 1991; Wickens, 1994; Wickens and Bouma, 2000; Johnson et al., 2001; Hodgson et al., 2006; Prélat et al., 2009). Fan 4 is up to 65 m thick (Wickens and Bouma, 2000; Johnson et al., 2001) and is built of three sand-rich lobe complexes (LC1, 3, 5) that are separated by thin-bedded deposits of lobe complex fringes (LC2, 4; Spychala et al., 2017a). Palaeocurrents and thickness distributions indicate sediment transport to the north and northeast (Wickens and Bouma, 2000; Hodgson et al., 2006; Spychala et al., 2017a). Measured sections from outcrops and cores from strategically chosen locations (Fig. 1b) permitted a comprehensive data set with a 3D constraint on the geographical distribution of hybrid beds to be established.

2.2 Laingsburg depocentre

The Laingsburg depocentre is located approximately 80 km southeast of the Tanqua depocentre, adjacent to the Swartberg branch of the Cape Fold Belt (Fig. 1a, c). The proximal basin-floor system of the Laingsburg Formation is subdivided into Unit A (Sixsmith et al., 2004; Prélat and Hodgson, 2013; Hofstra et al., 2015; Spychala et al., 2017b) and Unit B (Grecula et al., 2003a; Brunt et al., 2013a; Fig. 2). Units A and B are separated by a 40 m thick hemipelagic mudstone, which contains a thin sand-prone unit referred to as the A/B Interfan (Grecula et al., 2003a; Flint et al. 2011; Fig. 2). The stratigraphy of Unit A was subdivided by Sixsmith et al. (2004) into seven sand-prone subunits called A.1 to A.7, separated by regional hemipelagic mudstone horizons. In agreement with Prélat & Hodgson (2013) and Spychala et al. (2017b), subunits A.4 and A.7 have been re-interpreted as lobe complexes within Subunits A.5 and A.6, respectively, as there is no true hemipelagic mudstone separating them. An overall progradational-aggradational-retrogradational stacking pattern trend has been identified (Sixsmith et al., 2004; Flint et al., 2011). Flint et al. (2011) reassessed the sequence stratigraphy of Unit A and suggested that the unit comprises three composite sequences. Subunits A.1 to A.3 together with the overlying mudstone form the first composite sequence. The second sequence marks the most basinward extension of sediment into the basin and consists of A.4, A.5, and the overlying hemipelagic mudstone. The third composite sequence marks an overall retrogradation and includes A.6, A.7, and the overlying 40 m thick mudstone. These three composite sequences make up the Unit A composite sequence set (Flint et al., 2011). The studied cores (BSL and Bav 1b; Fig. 1c) were obtained from research boreholes in the 'Skeiding' area within the post-depositional Baviaans syncline.

3. Methodology

For this study, 23,068 beds were individually assessed by their bed type (turbidite, hybrid bed, debrite). No distinction between different hybrid bed types was established as the overall distribution of these deposits is studied here. More detailed studies in the distribution of different hybrid bed types could be the scope of further investigations. The percentage of hybrid beds within subunits and lobe complexes was established in two ways: 1) as percentage of total number of events; and 2) as percentage of bulk thickness of stratigraphic unit. To determine the geographical distribution of hybrid beds ~11,000 beds from Tanqua Fan 4 were evaluated from four research wells (OR, KK, BK and GBE; see Fig. 1b) and outcrop data. The deposits of Fan 4 were examined on a lobe complex scale. Evaluation was limited to the basal three lobe complexes (LC1, LC2 and LC3) as these are extensive across the whole study area (Spychala et al. 2017a). Additionally, their palaeogeography is well constrained (cf. Hodgson et al., 2006; Spychala et al., 2017a). To evaluate stratigraphic trends in hybrid bed distribution, ~12,000 beds of the BSL and Bav1b cores (Laingsburg depocentre; see Fig. 1c) were examined. The core locations are 1.58 km apart, and Bav1b is located obliquely down-dip of BSL. Bed type distribution was established for subunits A.1 - A.6 in both research boreholes. To compare bed distribution trends on a lobe complex scale in BSL and Bav1b, moving averages of bed types were established for subunits A.2 and A.3. For this purpose, the logged sections were divided into equal stratigraphic windows of 0.1 m thickness and the proportion of each bed type (turbidite, hybrid bed, debrite, siltstone and claystone) in these windows recorded. A moving average of each bed type throughout the well sequence was then derived from the average of a one metre window (ten 0.1 m sections). As the window moves up the succession in 0.1 m increments the average at step was calculated as a new value entered.

4. Bed types

Below a short description of the detailed facies of each sandstone bed type, turbidite, hybrid bed or debrite, is provided. Sedimentary facies and related environments of deposition have been described in detail previously for the Skoorsteenberg Formation (e.g. Morris et al., 2000; Johnson et al., 2001; van der Werff & Johnson, 2003a; Hodgson et al., 2006; Luthi et al., 2006; Prélat at al., 2009; Hodgson, 2009, Jobe et al., 2012; Hofstra et al., 2015; Spychala et al., 2017a) and the Laingsburg Formation (e.g. Grecula et al., 2003a, b; Sixsmith et al., 2004; Prélat and Hodgson, 2013; Hofstra et al., 2015; Spychala et al., 2017b).

4.1 Turbidites

Description. Turbidites include structureless sandstone, structured sandstone, banded sandstone and siltstones (Fig. 3a-g) that generally have a weak normal grading with tool marks where in contact with a mudstone at their base. In most cases, an individual turbidite bed shows more than one sedimentary facies with vertical and lateral transitions. Structureless sandstones are medium- to thick-bedded (>0.2 to 2 m), moderately to well sorted and upper fine- to lower fine-grained (Fig. 3a, e). Bed bases are sharp, erosive (with or without rip-up clasts present), amalgamated, or loaded and commonly show flute and tool marks. Beds can show weak normal grading, passing to very fine-grained sandstone at bed tops.

Structured sandstones are thin- to medium-bedded (0.1 to 0.7 m), very fine to fine-grained and well sorted. They display a range of laminated sedimentary structures (Fig. 3b, f). These include planar lamination, current-ripple lamination, climbing-ripple lamination and rarely wavy laminations. Current-ripple lamination foresets may have silt laminae drapes. Commonly, climbing-ripple lamination displays a low angle of climb and stoss-side preservation.

The differentiation between planar-laminated and banded facies is based on the thickness and character of the laminae. Banded sandstones are thin- to thick-bedded (0.1 to 1.5 m) and display alternating light and dark bands (Fig. 3c). The darker bands are 1 to 30 mm thick and poorly sorted, either more argillaceous or rich in mud chips and organics and in rare cases show a higher proportion in clay and silt matrix. The lighter ‘bands are cleaner and better sorted and commonly load into the darker bands.

Siltstones are very thin- to thin-bedded (0.01 to 0.2 m) and fine to coarse grained. They are structureless, planar laminated or current-ripple laminated (Fig. 3d, g) where siltstones show a sandier character Siltstones commonly show bioturbation.

Interpretation. Medium- to thick-bedded structureless sandstones are interpreted to be high-density turbidity currents deposits (Kneller and Branney, 1995) with high aggradation rates (Arnott and Hand, 1989; Leclair and Arnott, 2005; Talling et al., 2012a), which act to suppress the formation of sedimentary structures.

Structured thin- to medium-bedded sandstones are interpreted to be low-density turbidity currents deposits. Planar and current-ripple lamination are produced by reworking through dilute flows along the bed (Allen, 1982; Southard, 1991; Best and Bridge, 1992). Climbing-ripple lamination forms under bedload transport associated with high aggradation rates (Allen, 1973; Hunter, 1977; Jobe et al., 2012; Talling et al., 2012a). Wavy or sinusoidal lamination indicate deposition from waning currents with very high rates of suspension fallout (Allen, 1973; Jopling and Walker, 1968; Hunter, 1977).

Banded sandstones are interpreted to be deposited by transitional flows. Fluctuations of clay content of near-bed layers result in flows alternating between fully turbulent and more cohesive viscous types, thereby depositing alternating clean and argillaceous sand laminae (Lowe and Guy 2000; Davis et al. 2009; Haughton et al. 2009).They are comparable to the H2 division of Haughton *et al*. (2009), and represent <0.5% of the total facies by of events.

Although banded sandstones are not deposited by fully turbulent flows (Lowe and Guy 2000; Hofstra et al. 2015), they are included in the turbidite category for the purpose of this study as these deposits occur dominantly as top divisions of structureless sandstone beds, and not in association with an overlying debritic division.

Thin-bedded siltstones are interpreted to be dilute turbidity currents deposits. Planar lamination is a product of traction (Stow and Piper, 1984; Mutti, 1992; Talling et al., 2012a). Structureless beds are formed by direct suspension fallout (Bouma, 1962).

4.2 Hybrid beds

Description. Hybrid beds are thin- to thick-bedded (0.05 to 1.5 m) and include a lower and upper division (Fig. 4). The lower division is well-sorted, fine- to very fine-grained, commonly structureless and dewatered sandstone that can have a sharp, loaded or erosive base. Rip-up clasts at the base and dewatering features are common. Mudstone chips (up to 10% in volume) can occur towards the top of the lower division. The upper division is 1) argillaceous, poorly sorted sandstone with a swirly and patchy fabric comprising mudstone chips and carbonaceous material (carbonaceous hybrid beds, cf. D1 of Hodgson, 2009); or 2) argillaceous, micaceous, poorly sorted, mudstone/siltstone clast-rich sandstone with outsized grains compared to the overall grain size of the bed (clast-rich hybrid beds, cf. D2 of Hodgson, 2009). Characteristically, the fabric is swirly and patchy. Mudstone and siltstone clasts and fragments show no preferred orientation. In rare cases, the upper division can be mudstone clast-rich with a similar orientation and size in a well sorted sandstone matrix (cf. D3 of Hodgson, 2009).

Interpretation. Three models are invoked for the formation of hybrid beds (Talling, 2013). 1) Co-generation by independent flows: In this model independent debris flows and turbidity currents are developed by the failure of the slope and juxtaposed to form a bed with a clean sandstone division and a chaotic muddy division (Wood and Smith, 1958; Nelson et al., 1992; Masson et al., 1997). 2) Longitudinal evolution from a turbidity current (*sensu* Haughton et al. 2003). In this scenario part of a turbidity current undergoes flow transformation through the successive entrainment of mud-prone substrate that suppress turbulence, transforming a section of the flow to a laminar flow (Haughton et al., 2003; Talling et al., 2004; Ito, 2008; Davies et al., 2009; Haughton et al., 2009; Hodgson, 2009; Magalhaes and Tinterri, 2010; Patacci et al., 2014). 3) Vertical segregation in supersaturated flows (*sensu* Baas et al., 2009). In this model, a supersaturated turbidity current transforms into a quasi-laminar flow through vertical segregation of grains due to deceleration and increased flow concentration (Baas et al., 2009; Sumner et al., 2009; Baas et al., 2011; Kane and Pontén, 2012; Kane et al., 2017).. The resulting enhanced flow stratification leads to the development of a dense, cohesive basal layer (e.g., McCave and Jones, 1988; Kane and Pontén, 2012; Talling, 2013; Kane et al., 2017) and the suppression of upward turbulence transfer, eventually resulting in the collapse of the upper part of the flow (McCave and Jones 1988; Kane et al., 2017; Spychala et al., 2017a).

As most hybrid beds in the unconfined lobes of the Tanqua and Laingsburg depocentre show abrupt pinch-outs of both the lower and upper parts of hybrid beds the model of flow collapse is the favoured process interpretation for the majority of hybrid beds documented (Kane et al. 2017; Spychala et al. 2017a). Longitudinal evolution (model 2), whereby the flow fractions into a forerunning turbidity currents with trailing debris flows (Haughton et al., 2003, 2009) may account for thicker debrites found in the frontal pinch-out fingers (Hodgson 2009). Rare hybrid beds with an upper clast-rich division with a well-sorted sand matrix are interpreted to be formed as a suspension deposit from a turbidity current (Hodgson, 2009).

4.3 Debrites

Debrites are thick- to thin-bedded (3.0 to 0.2 m), poorly sorted argillaceous sandstones with outsized quartz grains (upper fine sand). Their fabric is swirly and patchy. Commonly, these deposits comprise variable amounts of mudstone and siltstone clasts (<1 and 35 cm in diameter), and carbonaceous material that show no preferred orientations.

Debrites are interpreted to be deposited by *en-masse* freezing of debris flows (Iverson, 1997; Talling et al., 2012b; Talling, 2013). Some isolated debrites may be the debritic divisions of hybrid beds that have out-run their basal turbidite.

5. Lobe hierarchy

Several studies have proposed that successions of sand-prone submarine lobes can be subdivided using a hierarchical approach (Gervais et al., 2006; Deptuck et al., 2008, Saller et al., 2008; Prélat et al., 2009; Mulder and Etienne, 2010; Prélat et al., 2010; Bernhard et al., 2012; Etienne et al., 2012; Grundvåg et al., 2014). Commonly, these successions are separated by regional hemipelagic mudstones that mark shutdown in coarse clastic sediment supply to the deep basin, and are interpreted to represent transgressive and highstand systems tracts (Flint et al. 2011). A fourfold hierarchy of lobe deposits in the Karoo Basin was established by Prélat et al. (2009) where 1) a 'bed' represents a single depositional event; 2) one or more beds form a 'lobe element'; 3) one or more lobe elements form a 'lobe'; 4) one or more genetically related lobes stack to form a 'lobe complex'. This hierarchy was extended to include a fifth hierarchical unit, the 'lobe complex set', which is formed by one or more genetically related lobe complexes within the same lowstand systems tract (Spychala et al., 2017a). Sand-prone lobe complexes are between 20-50 m thick and separated by several metre thick thin-bedded siltstone-prone packages, interpreted as the fringes of lobe complex (Prélat and Hodgson, 2013; Spychala et al., 2017a). Criteria used to identify individual lobes include sandstone-prone packages abruptly bounded by 0.2 - 1.5 m thick thin-bedded siltstone packages (< 20% sandstone). The thin-bedded siltstone packages are interpreted as distal lobe fringe deposits. The abrupt stratigraphic change in facies is interpreted to indicate avulsion of feeder channel, and compensational stacking of lobes (Prélat and Hodgson, 2013). Lobes are between 1 m (in distal environments) and 10 m (in axial environments) thick (Prélat et al. 2009, 2010). Mapping of individual lobes has established environments of deposition, although these are transitional in dip and strike sections (Spychala et al. 2017a). Thick-bedded deposits with a major proportion of structureless sandstone are interpreted to represent a lobe axis environment. Laterally, these pass into a higher proportion of medium-bedded structured sandstone deposits interpreted as a lobe off-axis environment. Further thinning and fining into successions characterised by hybrid bed prone successions and packages of thin-bedded interbedded siltstones and sandstones are interpreted as frontal or lateral lobe fringes (Spychala et al., 2017a).

6. Results

The proportion of hybrid beds has been evaluated in two respects at different stratigraphic scales: 1) the percentage of hybrid beds in the total number of events, and 2) the percentage of hybrid beds in the cumulative thickness. In a first step, the proportion of hybrid beds was established on a subunit scale (Table 1), which are defined as sand-prone units encased by regional hemipelagic claystones and fine siltstone units, and may comprise one or more lobe complexes (i.e. a lobe complex set). In the subunits from the Tanqua and Laingsburg depocentre locations, the proportion of hybrid beds is below 5% (4% mean; 3% median).

Their percentage of bulk thickness averages 9.2% (8% median) with 90% of the values being below 33% of the succession thickness (Fig. 5b), which means that cumulative hybrid bed thickness rarely comprises more than a third of the total succession thickness. However, this crude evaluation does not take into account palaeogeographic differences of data or stratigraphic hierarchies. Therefore, in the following sections, studied successions have been subdivided into lobe complexes based on previous work (Prélat and Hodgson 2013; Spychala et al., 2017a, b).

7. Results

7.1 Geographical trend

The palaeogeography, stratigraphic architecture and facies of lobe complex 1 (LC1) of Fan 4 (Tanqua depocentre) is well established (Hodgson et al., 2006, their Fig. 13; Spychala et al., 2017a, their Figs. 6, 7 and 10). Sediment was supplied from the southwest and palaeoflow directions are to the north and northeast (Fig. 1). LC1 is ~25 m thick in the south (OR) and thins northward to 5 m (OC1-6; Sout Rivier) before it pinches out abruptly (OC 7). Therefore, a cross-section from south (OR) to north (OC 6) represents a proximal to distal trend (Fig. 6a). The percentage of hybrid beds is less than 10% in terms of total events that make up LC1, except for a spike (33.3%) in OC 4 (Fig. 5b). Deposits of OC 4 represent a frontal lobe fringe pinch-out finger; these deposits contain high proportion of hybrid beds (Spychala et al., 2017a). There is a parallel trend in the bulk thickness of hybrid beds in LC1 (Fig. 6c) from 2.1% to 83.3% (Table 1) from the proximal to distal areas of the lobe complex followed by an abrupt decrease.

7.2 Stratigraphic trends

Unit A of the Laingsburg Formation comprises six subunits (Sixsmith et al., 2004; Prélat and Hodgson, 2013; Spychala et al., 2017b) that are separated by intervals of siltstone and hemipelagic mudstone that have been mapped regionally (Flint et al., 2011). Subunits A.2 and A.3 of Laingsburg Fan A each comprise one lobe complex in the study area, whereas Subunits A.1, A.5 and A.6 comprise two to eight lobe complexes (A.1.1-3; A.5.1-8; A.6.1-2; see Fig. 7). Due to the well-established stratigraphy, the core from research boreholes BSL and Bav1b (Fig. 1) are well suited for the evaluation of the stratigraphic distribution of hybrid beds.

Hybrid beds account for < 10% of beds in all subunits in both locations (Table 1). However, evaluation of their proportion of bulk thickness shows that there are considerable variations between the subunits (Table 1). In the BSL core, A.1 comprises 7.7% hybrid beds, A.2 slightly less (4.9%), whereas there is 30.2% in A.3. Subunits A.5 and A.6 contain 8.5% and 8.2% of hybrid beds, respectively. In the Bav1b core, the largest bulk thickness is A.1 (17.9%) and A.2 (18.2%). The proportion decreases significantly in A.3 (6.3%), and subunits A.5 and A.6 (both 6.9%) (Table 1).

The subunits have been subdivided into sand-prone lobe complexes and metres thick thin-bedded heterolithic packages that are interpreted as the fringes to lobe complexes (cf. Prélat et al., 2009; Prélat and Hodgson, 2013; Spychala et al., 2017a). These data suggest: i) there is no clear stratigraphic trend in hybrid beds at the scale of the composite sequence set (Flint et al., 2011), which show a high number of events in A.5.5 for both cores, whereas in cumulative thickness they are most prevalent in A.3 of the BSL core and A.1.1 in the Bav1b core (Table 1); ii) the younger lobe complexes (A.5.5- A.6.2) show an in-phase occurrence of hybrid beds for both cores; iii) the two lobe complexes of A.6 are the only intervals that show the same trends in the occurrence and thickness of hybrid beds in both cores; and iv) hybrid beds are a minor component of the lobe complex fringe successions, and comprise less than 2% of events and bulk thickness (Fig. 8).

Sub-units A.2 and A.3 show a marked difference in hybrid bed distribution between the two locations (BSL and Bav1b; Fig. 1), and this lateral variability is examined in more detail (Figs. 9 a-c). For this purpose, moving averages for bed types in sequential 1 m windows have been established and aligned with the corresponding core log (Fig. 9). The base and top of both A.2 and A.3 are rich in hybrid beds in both cores, however there are differences in the spatial distribution of hybrid beds. The Unit A.2 lobe complex shows an increased proportion of hybrid beds from BSL to Bav1b, whereas A.3 lobe complex shows a decrease in hybrid bed proportion from BSL to Bav1b. Hybrid beds occur throughout the succession, either irregularly as in A.3 at BSL (Fig. 9b) or regularly as in A.3 at Bav1b (every ~10m; Fig. 9c). Commonly, there is a higher proportion of hybrid beds at the base and top of the A.2 and A.3 lobe complexes (Fig. 10), with the exception of lobe complex A.3 of the BSL core. Here, the majority of hybrid bed events occur in the middle part of the lobe complex succession (Fig. 10).

8. Discussion

8.1 Proximal to distal trend

A strong geographic trend is evident in LC1 of Fan 4, showing that hybrid bed occurrence increases towards the frontal fringes of a lobe complex (up to 30% of events and > 50% of deposit thickness; Fig. 6b,c), before their proportion drops abruptly towards the sand pinch-out (Fig. 6b,c). In contrast, lateral thin-bedded lobe fringes (Fig. 8) contain less than 2% of hybrid beds. Recent studies (Kane et al., 2017; Spychala et al., 2017a) that show hybrid beds are also more prevalent in the frontal fringes of individual lobes suggest that similar trends can be evoked for several scales of hierarchy. The distinctly different distribution between frontal and lateral fringes has been interpreted to be caused by the spatial distribution of primary flow processes (Spychala et al. 2017a). High-density turbidity currents that can transform to co-genetic flows are transported farther out to the frontal fringes of the lobes, whereas low-density turbidity currents that deposit structured thin-beds spread out more radially and build up the lateral fringes. This study has quantified the previously qualitative observation that hybrid beds are preferentially found in the distal parts of lobe complexes (Ito, 2008; Hodgson, 2009; Pyles and Jennette, 2009; Talling et al., 2012a; Etienne et al., 2012a; Kane and Pontén, 2012; Grundvåg et al., 2014; Collins et al., 2015; Fonnesu et al., 2015, 2017; Pierce et al., in review).

8.2 Stratigraphic distribution within Unit A

Data from Unit A show there is an unorganised stratigraphic distribution of hybrid beds at the scale of a composite sequence set. Hybrid beds are less common in the basal (A.1) and top (A.6) subunits in both core data sets (cf. Table 1) compared to A.2-A.5 (Fig. 11). These results contrast with the simple model of hybrid bed distribution that has been proposed by several authors (e.g. Haughton et al., 2003, 2009; Hodgson, 2009) that predict hybrid beds are most common in the basal part of deep-water successions during fan (lobe complex or lobe complex set) initiation and growth. The rationale being that the generation of hybrid beds is associated with the disequilibrium of steep, out-of-grade muddy slopes that would achieve equilibrium over the period of sediment accumulation on the basin-floor fan. Less muddy material, needed to induce longitudinal flow transformation, would be entrained through time; therefore, hybrid beds are predicted to be less common in the younger parts of successions (*sensu* Haughton et al., 2009).

Haughton et al. (2009) suggested that deviation from this simple model can be used to infer aspects of the evolution on the supply slope: i) occurrence of hybrid beds throughout a basin-floor system is connected to a supply slope that never achieved equilibrium; ii) sporadic occurrence through the system can point to intermittent periods where the slope is in disequilibrium due to slope adjustments caused by tectonics (cf. Tinterri and Tagliaferri, 2015), intrabasinal topographic highs and depocentres with slope changes (Maghalaes and Tinterri, 2010) or changes in sediment supply. Van der Merwe et al. (2014) and Spychala et al. (2015) report a stepped slope profile that influenced the overlying Fort Brown Formation, while Spychala et al. (2017b) describe a dynamic intrabasinal slope that confined Unit A to the north. Therefore, the supply slope during the deposition of Unit A may have been stepped and/or dynamic meaning that the slope never reached equilibrium.

Another factor that has been shown to have influenced the distribution of hybrid beds is frontal basin confinement (e.g. Patacci et al., 2014; Southern et al., 2015), which leads to rapid flow expansion and deceleration. The lobe complexes of the Laingsburg depocentre are interpreted to have experienced minor to no confinement in their axes and subtle confinement to their lateral fringes (Sixsmith et al., 2004; Spychala et al., 2017b) therefore enhanced deceleration (Patacci et al., 2014, Southern et al., 2015) can be eliminated as a controlling factor on the stratigraphic distribution of hybrid beds, particularly in the Skeiding area (Fig. 1).

However, the paucity of clear stratigraphic trends at the scale of the composite sequence set suggests that there is a complicated interplay of factors involved in hybrid bed initiation and deposition. Flow transformation, from turbidity currents to flows that display fully turbulent and laminar behaviour, has been reported to occur when turbidity currents erode and entrain substrate material at the channel-lobe transition zone or on the basin-floor (Haughton et al., 2003, 2009; Hodgson, 2009, Fonnesu et al., 2016, 2017; Kane et al., 2017) leading to i) enhanced stratification and eventually to the collapse of the upper part of the flow (McCave and Jones, 1988; Kane and Pontén, 2012; Kane et al., 2017), or ii) longitudinal flow transformation to a co-genetic turbidity current and debris flow (Haughton et al., 2003; Talling et al., 2004; Ito, 2008; Davis et al., 2009; Haughton et al., 2009; Magahlaes &

Tinterri, 2010; Patacci et al., 2014). Fonnesu et al. (2017) and Pierce et al. (in review) pointed out that hybrid beds could form by a range of mechanisms even in the same system. This could explain why the distribution in the composite sequence set of Unit A of the Laingsburg Formation is not explainable with a model that only considers the state of the supply slope.

8.3 Stratigraphic distribution on the scale of a lobe complex

The bases and tops of lobe complexes A.2 and A.3 are observed to be slightly enriched in hybrid beds, although there is little discernible repeatable pattern in the distribution of hybrid beds through these lobe complexes (Fig. 10), whereas lobe complexes A.5.1, A.5.5 and A.6.1 show no occurrence of hybrid beds on their bases. The initiation of a new lobe complex is interpreted to mark a major avulsion of the feeder channel (Prélat and Hodgson 2013). For example, Picot et al. (2016) suggest that channel avulsion is an important factor that can disrupt the equilibrium profile and is connected to the deposition of lobe complex successions. Ortiz-Karpf et al. (2015) inferred less sandy lobes early during a channel avulsion from seismic amplitude responses due to entrainment of mud before new feeder channels could be established. This aligns with Terlaky et al. (2016) who interpret argillaceous sandstone splays (termed avulsion splays) to be associated with channel avulsion in proximal fan areas. High angle and up-dip channel avulsion could promote the occurrence of hybrid beds at the initiation phase of lobe complexes. If avulsion was a major factor governing the distribution of hybrid beds on a lobe complex scale an abundance of hybrid beds in their basal intervals would be predicted as this process is coupled with enhanced erosion into muddy substrate. However, the occurrence of erodible hemipelagic claystones between lobe complexes do not seem to have a major impact on the proportion of hybrid beds. For example, lobe complex A.5.5 shows the highest amount of hybrid bed flow events , but is underlain by a silt-prone lobe complex fringe (A.5.4; cf. Fig. 8) and the observed hybrid beds are not concentrated at the base of this lobe complex.

Although, the contribution of up-dip erosion into muddy substrate as factor for the enrichment of hybrid beds in the bases of lobe complexes cannot be excluded, it does not explain the fact that enrichment of hybrid beds is also observed from the top of lobe complexes. Therefore, we propose that the observed pattern is due to stacking pattern of lobes within the lobe complexes. Lobes show the overall tendency to initially prograde into the unconfined basin and subsequently fill up available space by compensational stacking, before they eventually backstep (retrograde) at the end of a depositional cycle (Hodgson et al., 2006; Prélat et al., 2009; Grundvåg et al. 2014; Hodgson et al., 2016). This means that in a 1D-section of a lobe complex hybrid-rich lobes are prevalent at the base and top as these record their distal sub-environments (frontal fringes).

8.4 Stratigraphic distribution on the scale of a lobe

At the scale of lobes, hybrid beds can be observed in the following settings: i) thick- to medium bedded structureless and structured sandstone-prone lobes show rare and irregular occurrence of hybrid beds (lobe axis and lobe off-axis), ii) thin-to-medium bedded structureless and structured sandstone and siltstones deposits that are rich in hybrid beds (frontal lobe fringe; cf. Fig. 12 b, lobes 4 and 9), and iii) thin-to-medium bedded structured sandstone and siltstone deposits that are poor in hybrid beds (lateral lobe fringes; Fig. 12b, lobe 11). Although hybrid beds can be observed in all lobe sub-environments, they are most prevalent in frontal lobe fringes in terms of recorded events and thickness proportions (Figs. 6 and 12). The 1D-core data sets conform to the observation from outcrop studies with 3D control that lobes have two fringe types - hybrid bed-prone frontal fringes and hybrid bed-poor lateral fringes (Spychala et al. 2017a). In addition, it shows that the distribution in a 1D vertical succession reflects the 3D stacking of lobes and their sub-environments (Prélat and Hodgson, 2013, Fonnesu et al., 2017).

Although individual lobes can be enriched in hybrid beds, there is little discernible stratigraphic pattern (Fig. 12). Lobes are a composite deposit of lobe elements, which is well expressed in lobe 8 of Subunit A.3 in Figure 12 b. The lack of pattern is because lobe elements stack in a range of patterns (compensational, disorganized, laterally stacked, landward and basinward stepping; Prélat and Hodgson, 2013)). In addition, although Prélat et al. (2010) drew lobe elements as smaller versions of lobes, implying similar shapes and facies distributions, this has not be confirmed by primary field observations.

8.5 Lobe stacking patterns from 1D data

We propose that stratigraphic distributions of clean sandstones, thin-bedded heterolithic deposits and hybrid-bed prone deposits within a lobe complex is dependent on the dominant stacking patterns of lobes (aggradational, compensational, and longitudinal (progradational and retrogradational); Fig. 13) and reflects the spatial relationship of lobe sub-environments (Fig. 14a; cf. Fonnesu et al., 2017). The stratigraphic distribution of reservoir sandstones, and non-reservoir hybrid bed-prone and heterolithic deposits in 1D-data can be used to infer 3D lobe stacking patterns. Where aggradational stacking patterns dominate, and a core is sited in the axial area, few hybrid beds are predicted (Figs. 13 and 14b). However, if the succession is intersected in their frontal fringe, the strata would be hybrid bed-rich (Fig. 13c). If progradational stacking of lobes is dominant (e.g. Grundvåg et al. 2014), hybrid beds will be abundant on the base and become less frequent upwards in the succession (Figs. 13 and 14d).Retrogradational stacking patterns would display the opposite distribution with hybrid beds being abundant in the top interval of the succession (Fig. 13). However, when compensational stacking is the dominant stacking pattern (e.g. Picot et al., 2016; Fonnesu et al., 2017), reservoir and non-reservoir facies will be less predictable as lobe sub-environments are superimposed in a more complicated manner (Figs. 13 and14b).

A lobe complex can display more than one stacking pattern. For example, the progradational-aggradational-retrogradational stacking of lobes within a lobe complex (e.g. Hodgson et al., 2006; 2016) would result in older and younger lobes being hybrid bed-prone, while the aggradational middle section would show no or rare hybrid beds. This depends on the availability and capacity of the muddy substrate to be entrained in flows that deposit younger lobes. In cases like A.2 and A.3, for example, where hybrid beds are mostly stacked irregularly with slightly higher percentages in their base and top, a dominant compensational stacking can be inferred. Thus, the basin is interpreted to be relatively unconfined, which agrees with the reconstruction of the Laingsburg depocentre (van der Merwe et al. 2014). In the future, hybrid bed distribution in a 1D data set could be used to form an initial evaluation of the dominant stacking pattern of lobes within a system (Fig. 13), and from this the degree of confinement at the time of deposition could be estimated.

9. Conclusions

Hybrid beds are a key heterogeneity in basin-floor fans, and predicting their stratigraphic and geographic distribution is important in subsurface reservoir investigations. A well-constrained outcrop and core data set from two unconfined basin-floor fans of the Karoo Basin, South Africa, have permitted the stratigraphic and geographic distribution of hybrid beds to be constrained quantitatively. On average, hybrid beds represent 4% of all beds (9.2% of cumulative thickness) within the database. There is a strong geographic trend showing that while hybrid beds occur throughout lobes, they are preferentially found in frontal lobe fringes (up to 33% of the total number of events and 83% of deposit thickness), while there is a paucity of hybrid beds in the lateral lobe fringes (<2%). Stratigraphic trends do not support allogenic controls, such as basin confinement, nature of the supply slope, and sediment supply cycles, as the main factors on the generation and distribution of hybrid beds in lobe complexes. The occurrence and distribution of hybrid beds is interpreted to be controlled by autogenic processes, such as channel avulsion, flow transformation processes on the basin-floor, and the stacking patterns of lobes in lobe complexes. Stacking patterns of lobes can be inferred from the vertical distribution of hybrid beds in lobe complexes, which reflects the spatial relationship of lobe sub-environments, and could be indicative of the degree of confinement on the basin-floor at the time of deposition.

10. Acknowledgements

The authors would like to thank the local farmers of the Tanqua region of South Africa for permission to carry out field studies on their land. Further, we would like to thank Aurelia Privat for assistance in the field and the core store. Graham Botha is acknowledged for logistic help in the core store. The clarity of the manuscript was improved by constructive reviews from Marco Fonnesu and Julian Clark. The LOBE 2 consortium project, of which this research forms a part, is supported by sponsorship from Anadarko, Bayerngas Norge, BG Group, BHPBilliton, BP, Chevron, DONG Energy, ENGIE, Maersk, Marathon, Petrobras, Premier Oil, Shell, Statoil, Total, VNG Norge, and Woodside, for which the authors are grateful.

11. References

Allen, J.R.L., 1973. A classification of climbing-ripple cross-lamination. Journal of the Geological Society London 129, 537–541.

Allen, J.R.L., 1982. Sedimentary Structures: Their Character and Physical Basis, Vols. 1, 2. Amsterdam. Elsevier. 593pp., 663pp.

Amy, L.A., Peachey, S.A., Gardiner, A.A. and Talling, P.J., 2009. Prediction of hydrocarbon recovery from turbidite sandstones with linked-debrite facies: Numerical flow-simulation studies. Marine and Petroleum Geology, 26, 2032-2043

Arnott, R.W.C., Hand, B.C., 1989. Bedforms, primary structures and grain fabric in the presence of suspended sediment rain. Journal of Sedimentary Petrology 59, 1062-1069.

Baas, J.H. Best, J.L., Peakall, J., Wang, M., 2009. A phase diagram for turbulent, transitional, and laminar clay suspension flows. Journal of Sedimentary Research 79, 162-183.

Baas, J.H., Best, J.L., Peakall, J., 2011. Depositional processes, bedform development and hybrid bed formation in rapidly decelerated cohesive (mud-sand) sediment flows. Sedimentology 58, 1953-1987.

Bernhardt, A., Jobe, Z.R., Grove, M., Lowe, D.R., 2012. Palaeogeography and diachronous infill of an ancient deep-marine foreland basin, Upper Cretaceous Cerro Toro Formation, Magallanes Basin, Chile. Basin Research 24, 269-294.

Best, J., Bridge, J., 1992. The morphology and dynamics of low amplitude bedwaves upon upper stage plane beds and the preservation of planar laminae. Sedimentology 39, 737-752.

Bouma, A.H., 1962. Sedimentology of some flysch deposits: a graphic approach to facies interpretation. Elsevier, Amsterdam, 168p.

Bouma, A.H., Wickens, H.d.V., 1991. Permian passive margin submarine fan complex, Karoo Basin, South Africa: possible model to Gulf of Mexico. Gulf Coast Association of Geological Societies 41, 30-42.

Brunt, R.L., Hodgson, D.M., Flint, S.S., Pringle, J.K., Di Celma, C., Prélat, A., Grecula, M., 2013a. Confined to unconfined: Anatomy of a base of slope succession, Karoo Basin, South Africa. Marine and Petroleum Geology 41, 206-221.

Catuneanu, O., Hancox, P.J., Rubidge, B.S., 1998. Reciprocal flexural behaviour and contrasting stratigraphies: a new basin development model for the Karoo retroarc foreland system, South Africa. Basin Research 10, 417-439

Collins, J., Kenyon-Roberts, S., Cullen, B., White, J., Bordas-Le Floch, N., and Downey,J., 2015. Arran Field: a complex heterolithic reservoir on the margins of the Forties Fan System, in McKie, T., Rose, P.T.S., Hartley, A.J., Jones, D.W., and Armstrong, T.L., eds.,Tertiary Deep-Marine Reservoirs of the North Sea Region. Geological Society of London, Special Publication 403, 185–217.

Collinson, J.D., Martinsen, O., Bakken, B., Kloster, A., 1991. Early fill of the Western Irish Namurian Basin: a complex relationship between turbidites and deltas. Basin Research 3, 223-242.

Davis, C., Haughton, P., McCaffrey, W., Scott, E. Hogg, N., Kitching, D., 2009. Character and distribution of hybrid sediment gravity flow deposits from the outer Forties Fan, Palaeocene Central North Sea, UKCS. Marine and Petroleum Geology, 26, 1919-1939.

Deptuck, M.E., Piper, D.J.W., Savoye, B., Gervais, A., 2008. Dimensions and architecture of late Pleistocene submarine lobes off the northern margin of East Corsica. Sedimentology 55, 869-898.

Etienne, S., Mulder, T., Bez, M., Desaubliaux, G., Kwasniewski, A., Parize, O., Dujoncquoy, E., Salles, T., 2012. Multiple scale characterization of sand-rich distal lobe deposit variability: Examples from the Annot Sandstones Formation, Eocene–Oligocene, SE France. Sedimentary Geology 273-274, 1-18.

Feeley, M.H., Bufïler, R.T., Bryant, W.R., 1985. Depositional units and growth pattern of the Mississippi Fan. In: Bouma, A.H., Normark, W.R., Barnes, N.E. (Eds.), Submarine Fans and Related Turbidite Systems. 253–257.

Flint, S.S., Hodgson, D.M., Sprague, A.R., Brunt, R.L., van der Merwe, W.C., Figueiredo, J., Prélat, A., Box, D., Di Celma, C., Kavanagh, J. P., 2011. Depositional architecture and sequence stratigraphy of the Karoo basin floor to shelf edge succession, Laingsburg depocentre, South Africa. Marine and Petroleum Geology 28, 658-674.

Fonnesu, M., Haughton, P., Felletti, F., McCaffrey, W., 2015. Short length-scale variability of hybrid event beds and its applied significance. Marine and Petroleum Geology 67, 583-603.

Fonnesu M., Patacci, M., Haughton, P.D.W., Felletti, F., McCaffrey, W.D., 2016. Hybrid event beds generated by local substrate delamination on a confined-basin floor. Journal of Sedimentary Research 86, 929-943.

Fonnesu, M., Felletti, F., Haughton, P.D.W., Patacci, M., McCaffrey, W.D., 2017. Hybrid event bed character and distribution linked to turbidite system sub-environments: The North Apennine Gottero Sandstone (north-west Italy). Sedimentology (published online). DOI: 10.1111/sed.12376

Georgiopoulou, A., Wynn, R., Masson, D.G., Frenz, M., 2009. Linked turbidite-debrite resulting from recent Sahara Slide headwall reactivation. Marine and Petroleum Geology 26, 2021–2031.

Gervais, A., Savoye, B., Mulder, T., Gonthier, E., 2006. Sandy modern turbidite lobes: A new insight from high resolution seismic data: Marine and Petroleum Geology 23, 485-502.

Grecula, M., Flint, S.S., Wickens, H.D.V., Johnson, S.D., 2003a. Upward-thickening patterns and lateral continuity of Permian sand-rich turbidite channel fills, Laingsburg Karoo, South Africa. Sedimentology 50, 831-853.

Grundvåg, S.A., Johannessen, E.P., Helland-Hansen, W., Plink-Björklund, P., 2014. Depositional architecture and evolution of progradationally stacked lobe complexes in the Eocene Central Basin of Spitsbergen. Sedimentology 61, 535-569.

Haughton, P.D.W., Barker, S.P., McCaffrey, W.D., 2003. 'Linked' debrites in sand-rich turbidite systems – Origin and significance. Sedimentology 50, 459-482.

Haughton, P., Davis, C., McCaffrey, W., Barker, S., 2009. Hybrid sediment gravity flow deposits – Classification, origin and significance. Marine and Petroleum Geology 26, 1900-1918.

Hodgson, D.M., Flint, S.S., Hodgetts, D., Drinkwater, N.J., Johannessen, E.P., Luthi, S., 2006. Stratigraphic evolution of fine-grained submarine fan systems, Tanqua depocentre, Karoo Basin, South Africa. Journal of Sedimentary Research 76, 20– 40.

Hodgson, D.M., 2009. Distribution and origin of hybrid beds in sand-rich submarine fans of the Tanqua depocentre, Karoo Basin, South Africa. Marine and Petroleum Geology 26, 1940-1956.

Hodgson, D.M., Kane, I.A., Flint, S.S., Brunt, R.L., Ortiz-Karpf, A., 2016. Time-transgressive confinement on the slope and the progradation of basin-floor fans: Implications for the sequence stratigraphy of deep-water deposits.Journal of Sedimentary Research 86, 73-86.

Hofstra, M., Hodgson, D.M., Peakall, J., Flint, S.S., 2015. Giant-scour fills in ancient channel-lobe transition zones: Formative processes and depositional architecture. Sedimentary Geology 329, 98-114.

Hunter, R.E., 1977. Terminology of cross-stratified sedimentary layers and climbing-ripple structures. Journal of Sedimentary Research 47, 697–706.

Ito, M., 2008. Downfan transformation from turbidity currents to debris flows at a channel-to-lobe transitional zone: The lower Pleistocene Otadai Formation, Boso Peninsula, Japan. Journal of Sedimentary Research 78, 668-682.

Ito, M., Ishikawa, K., Nishida, N., 2014. Distinctive erosional and depositional structures formed at a canyon mouth: A lower Pleistocene deep-water succession in the Kazusa forearc basin on the Boso Peninsula, Japan. Sedimentology 61, 2042-2062.

Iverson, R.M., 1997. The physics of debris flow. Reviews of Geophysics 35, 245-296.

Jackson, C.A.-L., Zakaria, A.A., Johnson, H.D., Tongkul, F., Crevello, P.D., 2009. Sedimentology, stratigraphic occurrence and origin of linked debrites in the West Crocker Formation (Oligo-Miocene), Sabah, NW Borneo. Marine and Petroleum Geology 26, 1957-1973.

Jobe, Z.R., Lowe, D.R., Morris, W.R., 2012. Climbing-ripple successions in turbidite systems: depositional environments, sedimentation rates and accumulation times. Sedimentology 59, 867-898.

Jopling, A.V., Walker, R.G., 1968. Morphology and origin of ripple-drift cross-lamination, with examples from the Pleistocene of Massachusetts. Journal of Sedimentary Research 38, 971–984.

Johnson, S.D., Flint, S.S., Hinds, D., Wickens, H.d.V., 2001. Anatomy of basin floor to slope turbidite systems, Tanqua Karoo, South Africa: sedimentology, sequence stratigraphy and implications for subsurface prediction. Sedimentology 48, 987–1023.

Kane, I.A., Pontén, A.S.M., 2012. Submarine transitional flow deposits in the Palaeogene Gulf of Mexico. Geology 40, 1119-1122.

Kane, I.A., Pontén, A.S.M., Vangdal, B., Eggenhuisen, J.T., Hodgson, D.M., Spychala, Y.T., 2017. The stratigraphic record and processes of turbidity current transformation across deep-marine lobes. Sedimentology 64, 1236-1273.

Kneller, B.C., Branney, M.J., 1995. Sustained high-density turbidity currents and the deposition of thick massive sands. Sedimentology 42, 607-616.

Leclair, S.F., Arnott, R.W.C., 2005. Parallel lamination formed by high-density turbidity currents. Journal of Sedimentary Research 75, 1-5.

Lowe, D.R., 1982. Sediment gravity flows: II. Depositional models with special reference to the deposits of high-density turbidity currents. Journal of Sedimentary Petrology 52, 279-297.

Luthi, S.M., Hodgson, D.M., Geel, C.R., Flint, S.S., Goedbloed, J.W., Drinkwater, N.J., Johannessen, E.P., 2006. Contribution of research borehole data to modelling fine-grained turbidite reservoir analogues, Permian Tanqua-Karoo basin-floor fans (South Africa). Petroleum Geosciences 12, 175-190.

Masson, D.G., Van Niel, B., Waever, P.P.E., 1997. Flow processes and sediment deformation in the Canary Debris Flow on the NW African Continental Rise. Sedimentary Geology 110, 163-179.McCave, I.N., Jones, K.P.N., 1988. Deposition of ungraded muds from high-density non-turbulent turbidity currents. Nature 333, 250-252.

Magalhaes, P., Tinterri, R., 2010. Stratigraphy and depositional setting of slurry and contained (reflected) beds in the Marnoso-arenacea Formation (Langhian-Serravallian) Northern Apenninnes, Italy. Sedimentology 57, 1685-1720.

Morris, W.R., Scheilhing, M.H., Wickens, DeV., Bouma, A.H., 2000. Reservoir architecture of deepwater sandstones: examples from the Skoorsteenberg Formation, Tanqua Karoo Sub-Basin, South Africa. In: Weimer,P., Slatt, R.M., Bouma, A.H., Lawrence, D.T. (Eds.), Deep-water reservoirs of the world: Gulf Coast Section SEPM Foundation. Twentieth Annual Research Conference, 1010-1032.

Mulder, T., Etienne, S., 2010. Lobes in deep-sea turbidite systems: State of the art. Sedimentary Geology 229, 75-80.

Mutti, E., 1992. Turbidite Sandstones, Agip -Instituto di Geologia, Università di Parma, Italy, 275p.

Nelson, C.H., Twichell, D.C., Schwab, W.C., Lee, H.J., Kenyon, N.H., 1992. Upper Pleistocene turbidite sand beds and chaotic silt beds in the channelized, distal, outer-fan lobes of the Mississippi fan. Geology 20, 693–696.Ortiz-Karpf, A., Hodgson, D.M., McCaffrey, W.D., 2015. The role of mass-transport complexes in controlling channel avulsion and the subsequent sediment dispersal patterns on an active margin: The Magdalena Fan, offshore Colombia. Marine and Petroleum Geology 64, 58-75.

Patacci, M., Haughton, P.D.W., McCaffrey, W.D., 2014. Rheological complexity in sediment gravity flows forced to decelerate against a confining slope, Braux, SE France. Journal of Sedimentary Research 84, 270-277.

Picot, M., Droz, L., Marsset, T., Dennielou, B., Bez, M., 2016. Controls on turbidite sedimentation: Insights from a quantitative approach of submarine channel and lobe architecture (Late Quaternary Congo Fan). Marine and Petroleum Geology 72, 423-446.

Pierce, C.S., Haughton, P.D.W., Shannon, P.M., Pulham, A.J., Barker, S.P., Martinsen, O.J., in review. Variable character and diverse origin of Hybrid Event Beds (HEBs) in a sandy submarine fan system, Pennsylvanian Ross Sandstone Formation, western Ireland. Sedimentology xx, xxx-xxx

Porten, K.W., Kane, I.A., Warchoł, M.J., Southern, S.J., 2016. A sedimentological process-based approach to depositional reservoir quality of deep-marine sandstones: an example from the Springar Formation, Northwestern Vøring Basin, Norwegian Sea. Journal of Sedimentary Research 86, 1269-1286.

Prélat, A., Hodgson, D.M., Flint, S.S., 2009. Evolution, architecture and hierarchy of distributary deep-water deposits: a high-resolution outcrop investigation from the Permian Karoo Basin, South Africa. Sedimentology 56, 2132-2154.

Prélat, A., Covault, J.A., Hodgson, D.M., Fildani, A., Flint, S. S. 2010. Intrinsic controls on the range of volumes, morphologies, and dimensions of submarine lobes. Sedimentary Geology 232, 66-76.

Prélat, A., Hodgson, D.M., 2013. The full range of turbidite bed thickness patterns in submarine lobes: controls and implications. Journal of Geological Society of London 170, 1-6.

Pyles, D.R., Jennette, D.C., 2009. Geometry and architectural associations of co-genetic debrite–turbidite beds in basin-margin strata, Carboniferous Ross Sandstone (Ireland): Applications to reservoirs located on the margins of structurally confined submarine fans. Marine and Petroleum Geology 26, 1974-1996.

Pysklywec, R.N., Mitrovica, J.X., 1999. The role of subduction-induced subsidence in the evolution of the Karoo Basin. The Journal of Geology 107, 155-164.

Saller, A., Werner, K., Sugiaman, F., Cebastiant, A., May, R., Glenn, D., Barker, C., 2008. Characteristics of Pleistocene deep-water fan lobes and their application to an upper Miocene reservoir model, offshore East Kalimantan, Indonesia. AAPG Bulletin 92, 919–949.

Sixsmith, P.J., Flint, S.S., Wickens, H.D., Johnson, S.D., 2004. Anatomy and stratigraphic development of a basin floor turbidite system in the Laingsburg Formation, Main Karoo Basin, South Africa. Journal of Sedimentary Research 74, 239-254.

Southard, J.B., 1991. Experimental determination of bed-Form stability. Annual Review of Earth and Planetary Science 19, 423-55.

Southern, S.J., Patacci, M., Felletti, F., McCaffrey, W.D., 2015, Influence of flow containment and substrate entrainment upon sandy hybrid event beds containing a co-genetic mud-clast rich division. Sedimentary Geology 321, 105-122.

Southern, S.J., Kane, I.A., Warchoł, M.J., Porten, K.W. and McCaffrey, W.D., 2017. Hybrid event beds dominated by transitional-flow facies: Character, distribution and significance in the Maastrichtian Springar Formation, north-west Vøring Basin, Norwegian Sea. Sedimentology 64, 747-776.

Spychala, Y.T., Hodgson, D.M., Flint, S.S., Mountney, N.P., 2015. Constraining the sedimentology and stratigraphy of submarine intraslope lobe deposits using exhumed examples from the Karoo Basin, South Africa. Sedimentary Geology 322, 67-81.

Spychala, Y.T., Hodgson, D.M., Prélat, A., Kane, I.A., Flint, S.S., Mountney, N.P., 2017a. Frontal and lateral submarine fringes: Comparing sedimentary facies, architecture and flow processes. Journal of Sedimentary Research 87, 75-96.

Spychala, Y.T., Hodgson, D.M., Stevenson, C.J., and Flint, S.S., 2017b. Aggradational lobe fringes: the influence of subtle intrabasinal topography on sediment gravity flow processes and lobe stacking patterns. Sedimentology 64, 582-608.

Stow, D.A.V., Piper, D.J.W., 1984. Deep-water fine-grained sediments: facies models. In: Stow, D.A.V., Piper, D.J.W. (Eds.), Fine-grained Sediments: Deep-water Processes and Facies. Geological Society of London, Special Publication 15, 611-646.

Sumner, E.J., Amy, L.A., Talling, P.J., 2008. Deposit structure and processes of sand deposition from decelerating sediment suspensions. Journal of Sedimentary Research 79, 529-547.

Sumner, E.J., Talling, P.J., Amy, L.A., 2009. Deposits of flows transitional between turbidity current and debris flow. Geology 37, 991-994.

Tankard, A., Welsink, H., Aukes, P., Newton, R., Stettler, E., 2009. Tectonic evolution of the Cape and Karoo basins of South Africa. Marine and Petroleum Geology 26, 1379-1412.

Talling, P.J., Amy, L.A., Wynn, R.B., Peakall, J., Robinson, M., 2004. Beds comprising debrite sandwiched within co-genetic turbidite: origin and widespread occurrence in distal depositional environments. Sedimentology 51, 163-194.

Talling, P.J., Masson, D.G., Sumner, E.J., Malgesini, G., 2012a. Subaqueous sediment density flows: Depositional processes and deposit types. Sedimentology 59, 1937-2003.

Talling, P.J., Malgesini, G., Sumner, E.J., Amy, L.A., Felletti, F., Blackbourn, G., Nutt, C., Wilcox, C., Harding, I.C., and Akbari, S., 2012b, Planform geometry, stacking pattern, and extrabasinal origin of low strength and intermediate strength cohesive debris flow deposits in the Marnoso-arenacea Formation, Italy. Geosphere, 8, 1207-1230.

Talling, P.J., 2013. Hybrid submarine flows comprising turbidity current and cohesive debris flow: Deposits, theoretical and experimental analyses, and generalized models. Geosphere 9, 460-488.

Terlaky, V., Rocheleau, J. and Arnott, W.C., 2016, Stratal composition and stratigraphic organization of stratal elements in an ancient deep-marine basin-floor succession, Neoproterozoic Windermere Supergroup, British Columbia, Canada. Sedimentology 63, 136-175.

Tinterri, R. and Tagliaferri, A., 2015, The syntectonic evolution of foredeep turbidites related to basin segmentation: Facies response to the increase in tectonic confinement (Marnoso-arenacea Formation, Miocene, Northern Apennines, Italy). Marine and Petroleum Geology, 67, 81-110.

van der Merwe, W.C., Hodgson, D.M., Brunt, R.L., Flint, S.S., 2014. Depositional architecture of sand-attached and sand-detached channel-lobe transition zones on an exhumed stepped slope mapped over a 2500 km^2 area. Geosphere 10, 1076-1093.

van der Werff, W., Johnson, S., 2003a. High resolution stratigraphic analysis of a turbidite system, Tanqua Karoo Basin, South Africa: Marine and Petroleum. Geology 20, 45-69.

Visser, J.N.J., 1997. Deglaciation sequences in the Permo-Carboniferous Karoo and Kalahari basins of the southern Africa: a toll in the analysis of cyclic glaciomarine basin fills. Sedimentology 44, 507-521.

Visser, J.N.J., Prackelt, H.E., 1996. Subduction, mega-shear systems and Late Palaeozoic basin development in the African segment of Gondwana. Geologische Rundschau 85, 632-646.

Wickens, H.d.V., 1994. Basin floor fan building turbidites of the southwestern Karoo Basin, Permian Ecca Group. PhD Thesis, Port Elizabeth University, South Africa, 233pp.

Wickens, H.d.V., Bouma, A.H., 2000. The Tanqua Fan Complex, Karoo Basin, South Africa – outcrop analogue for fine-grained, deepwater deposits. In: Bouma, A.H., Stone, C.G. (Eds.), Fine-grained Turbidite Systems. AAPG Memoir 72/SEPM Special Publication 68, 153–165.

Wignall, P.B., Best, J.L., 2000. The Western Irish Namurian Basin reassessed. Basin Research 12, 59-78.

Wood, A., Smith, A.J., 1958. The sedimentation and sedimentary history of the Aberystwyth Grits (Upper Llandoverian). Quarterly Journal of the Geological Society 114, 163-195.

Figure Captions

Figure 1. A: Geological setting of the two study areas inboard of the two branches of the Cape Fold Belt; B: Schematic outline of the lower lobe complex of Fan 4 (Skoorsteenberg Formation, Tanqua depocentre and outcrop and core locations: OR, Ongeluksrivier; KK, Koppieskraal; BK, Bloukop; GBE, Gemsbok East; RW, Rondawell; OC1-7, Soutfontein 1-7; KF, Klipfontein; cf. Table 1); C: Schematic outline of Unit A and locations of the BSL and Bav1b cores. Outlines of A.2 and A.3 are modified after Sixsmith et al. (2004).

Figure 2. Stratigraphy of the Tanqua and Laingsburg depocentre; based on Wild et al. (2009) and Flint et al. (2011). The studied fan systems are highlighted with blue boxes and simplified zoom-ins provided. Zoom-in of the Laingsburg Formation modified from Sixsmith et al. (2004).

Figure 3. Representative photographs from outcrop and core for turbidite facies. A: Structureless sandstone, Rondawell, Fan 4, LC 3. Logging pole (10 cm increments) as scale. B: Ripple laminated sandstone, Klipfontein, Fan 4. Camera lens cover (7 cm diameter) as scale. C: Banded sandstone, Rietfontein (near BSL location outcrop), Subunit A.5. Compass as scale. D: Planar and ripple laminated siltstone, Klipfontein, Fan 4, LC 3. Logging pole (10 cm increments) as scale. E: Dewatered structureless sandstone, BSL core Subunit A.3. F: Ripple laminated sandstone, BSL core, Subunit A.5. G: Siltstone, BSL core, Subunit A.1.

Figure 4. Representative photographs of hybrid beds from outcrop and core. A: Hybrid bed (F4) with lower clean division and upper mudstone clast–rich division, Hammerkranz (south of RW), Fan 4, LC 1. Lens cover as scale (~7 cm diameter). B: Hybrid bed showing different weathering of lower clean and upper muddy division, Hammerkranz (south of RW), Fan 4, LC 1. Lens cover as scale (~7 cm diameter). C: Weathered mica-rich upper division with high mud content. Lens cover as scale (~7 cm diameter), Stegweeglagte, Subunit A.3. D: Hybrid bed. Upper clast rich division overlain directly by thin-bedded siltstone, Klipfontein, Fan 4, LC 1. Lens cover as scale (~7 cm diameter). E-G: Hybrid bed examples from core.

Figure 5 Hybrid bed distribution over the complete data set. A: Percentage of hybrid beds relative to all events. B: Hybrid bed proportion of the cumulative thickness

Figure 6. A: Schematic distribution of the outcrops over LC1. The green shading points out where hybrid beds are approximately 50% of the deposit thickness. B: Hybrid beds plotted as percentage of all flow events. C: Hybrid beds plotted as percentage of the bulk thickness of the succession

Figure 7. BSL core and gamma ray log showing the interpreted lobe complexes of Unit A.1 to A.6.

Figure 8. Hybrid bed distribution over the lobe complexes of Unit A. The graphs are linked to their depositional environment. The blue line displays values for BSL, whereas the violet line displays values for Bav1b.

Figure 9. A: Facies proportions of subunits A.1- A.2 of Unit A, Laingsburg Formation; B: Core log of Subunits A.2 and A.3 of the BSL core aligned with its bed type composition (moving average); C: Core log of Subunits A.2 and A.3 of the Bav1b core aligned with its bed type composition (moving average).

Figure 10. Distribution of hybrid beds through lobe complexes A.2 and A.3 for the BSL and Bav1b cores. The lobe complexes have been divided into three equal intervals and the proportion of the overall hybrid beds in these intervals was established.

Figure 11. Hybrid bed distribution curve for sand-prone lobe complexes of Unit A. The blue line displays values for BSL, whereas the violet line displays values for Bav1b.

Figure 12. Interpretation of individual lobes and their correlation from BSL to Bav1b. A: Correlation for the lobe complex of Subunit A.2. B: Correlation for the lobe complex of Subunit A.3.

Figure 13. Stacking patterns of lobe complexes and resulting hybrid bed distribution within an axial setting of a turbidite system reflecting temporal and spatial complexity as shown in 1D sections.

Figure 14. A: Distribution of hybrid beds in lobe fringes; B: Stochastic distribution of hybrid beds in a lobe complex due to compensational stacking patterns; C: Discrete areas of hybrid-bed rich and hybrid bed-poor successions in a lobe complex due to aggradational stacking; D: Marginal hybrid rich successions, axial hybrid bed clusters throughout the lobe complex due to longitudinal stacking.

898 Table 1. Proportion of hybrid beds for subunits of Unit A (BSL and Bav 1b; Laingsburg
899 depocentre) and lobe complexes 1-3 of Fan 4 (Skoorsteenberg Formation, Tanqua
900 depocentre.

Location	Subunit	% HB of total events	% HB of cumulative thickness
BSL	A.1	2	7.7
	A.2	4.7	4.9
	A.3	7.2	30.2
	A.5	4.5	8.5
	A.6	0.7	8.2
Bav 1b	A.1	2	17.9
	A.2	6.6	18.2
	A.3	3.5	6.3
	A.5	2.4	6.9
	A.6	0.4	6.9
OR1	Lower Fan 4	1.2	2.1
	Upper Fan 4	14.5	11.3
KK1	Lower Fan 4	3.2	16.3
	Upper Fan 4	12	23.7
BK1	Lower Fan 4	7.4	22.2
	Upper Fan 4	5.8	8.5
GBE	Lower Fan 4	4	34.1
	Upper Fan 4	2.9	11
RW2	Lower Fan 4	8.2	29.1
	Upper Fan 4		
OC2	Lower Fan 4	5.9	49.1
	Upper Fan 4	11.6	19.5
OC3	Lower Fan 4	3.4	40.9
	Upper Fan 4	18.2	19.2
OC4	Lower Fan 4	33.3	83.3
	Upper Fan 4	4.2	4
OC5	Lower Fan 4	1.8	26.1
	Upper Fan 4		
OC6	Lower Fan 4	2.2	4.8
	Upper Fan 4	7.8	8
KF1	Lower Fan 4	6.8	21.1
	Upper Fan 4	4.2	6.1
KF2	Lower Fan 4	4	2.9
	Upper Fan 4	0.6	1.1
KF3	Lower Fan 4	3.8	2.4
	Upper Fan 4		
KF4	Lower Fan 4	4.6	21.5
	Upper Fan 4	5.5	5.5
VF	Lower Fan 4	0	0
	Upper Fan 4	1.8	2.7

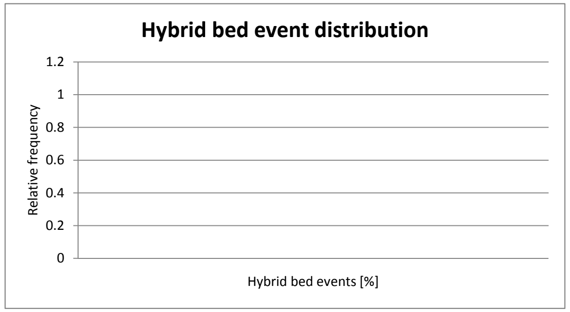

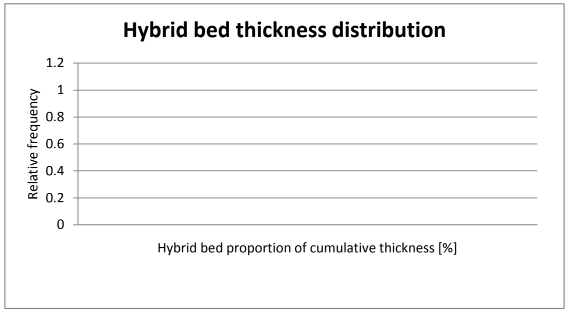

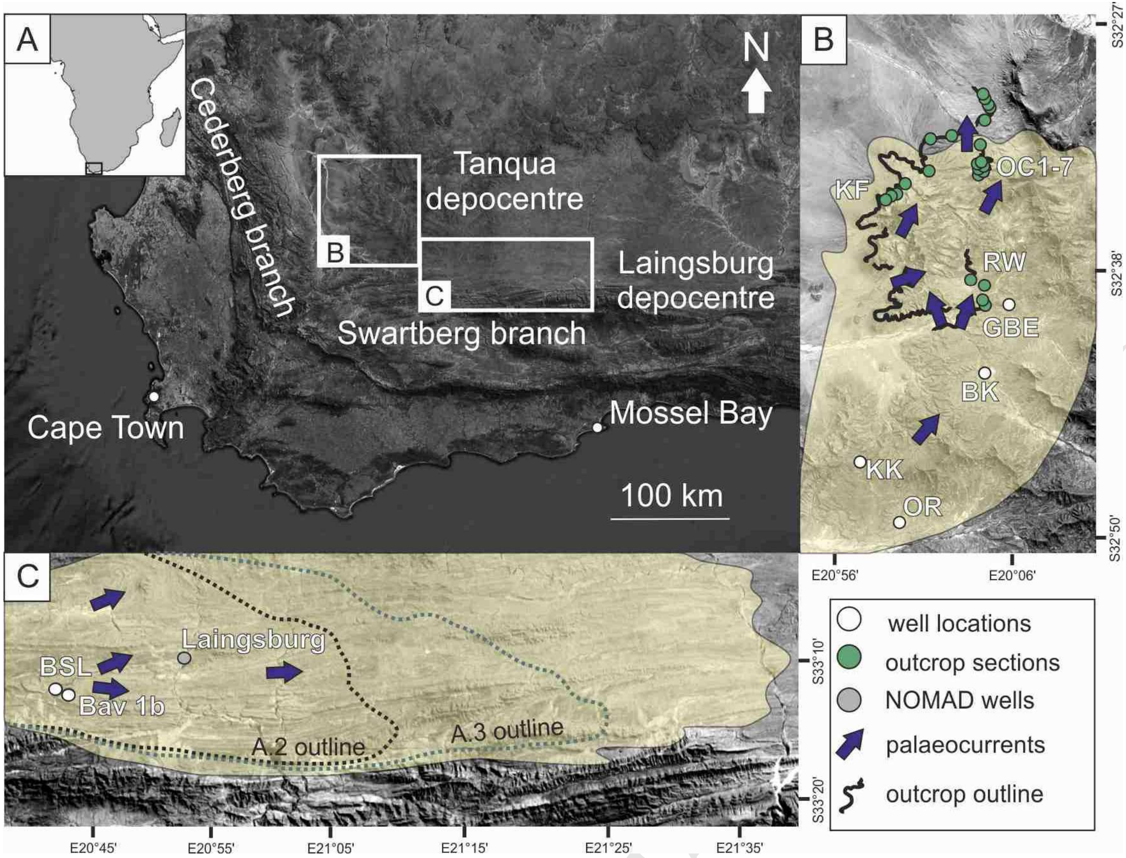
A
N
B
Cederberg branch
Tanqua depocentre
Laingsburg depocentre
Swartberg branch
Cape Town
Mossel Bay
100 km
KF
OC1-7
RW
GBE
BK
KK
OR
S32°27'
S32°38'
S32°50'
E20°56'
E20°06'
C
Laingsburg
BSL
Bav 1b
A.2 outline
A.3 outline
S33°10'
S33°20'
E20°45'
E20°55'
E21°05'
E21°15'
E21°25'
E21°35'
well locations
outcrop sections
NOMAD wells
palaeocurrents
outcrop outline

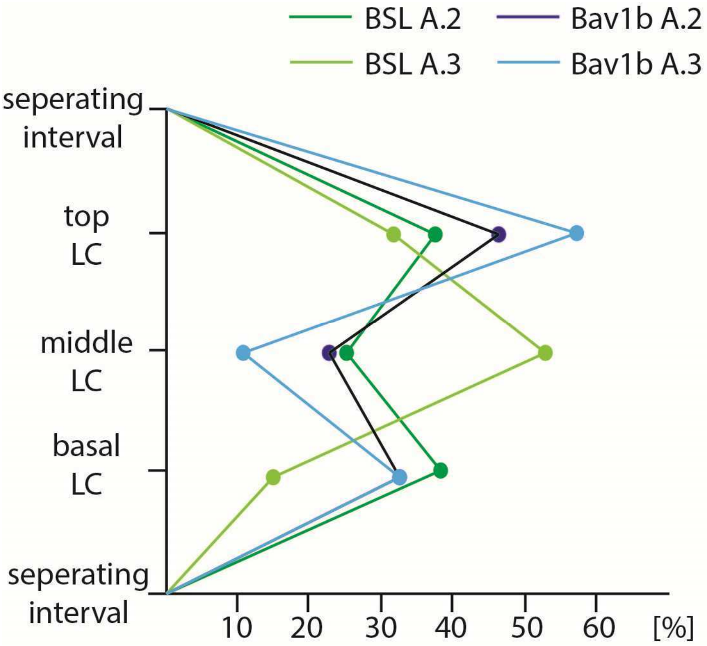
BSL A.2
Bav1b A.2
BSL A.3
Bav1b A.3
seperating interval
top LC
middle LC
basal LC
seperating interval
10
20
30
40
50
60
[%]

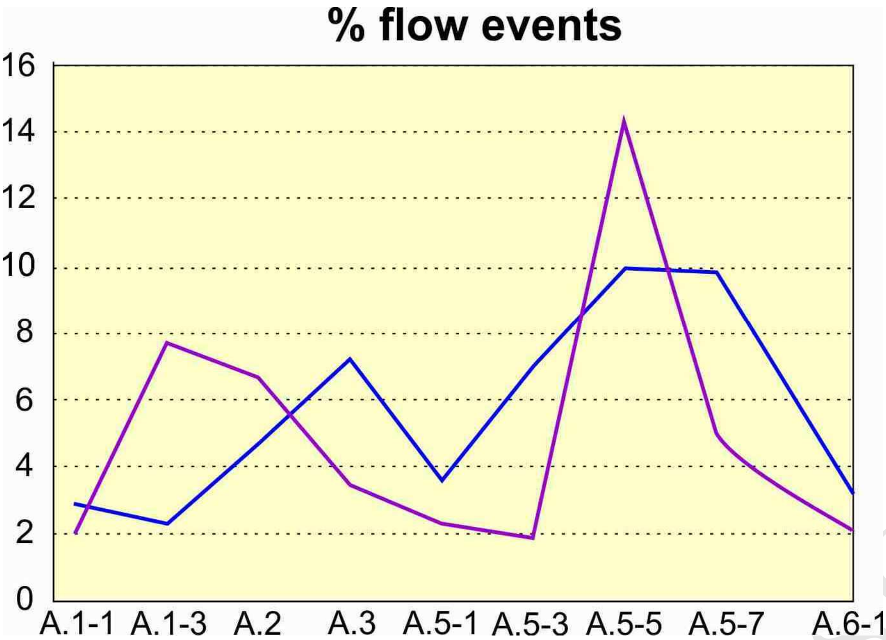

% flow events
16
14
12
10
8
6
4
2
0
A.1-1
A.1-3
A.2
A.3
A.5-1
A.5-3
A.5-5
A.5-7
A.6-1

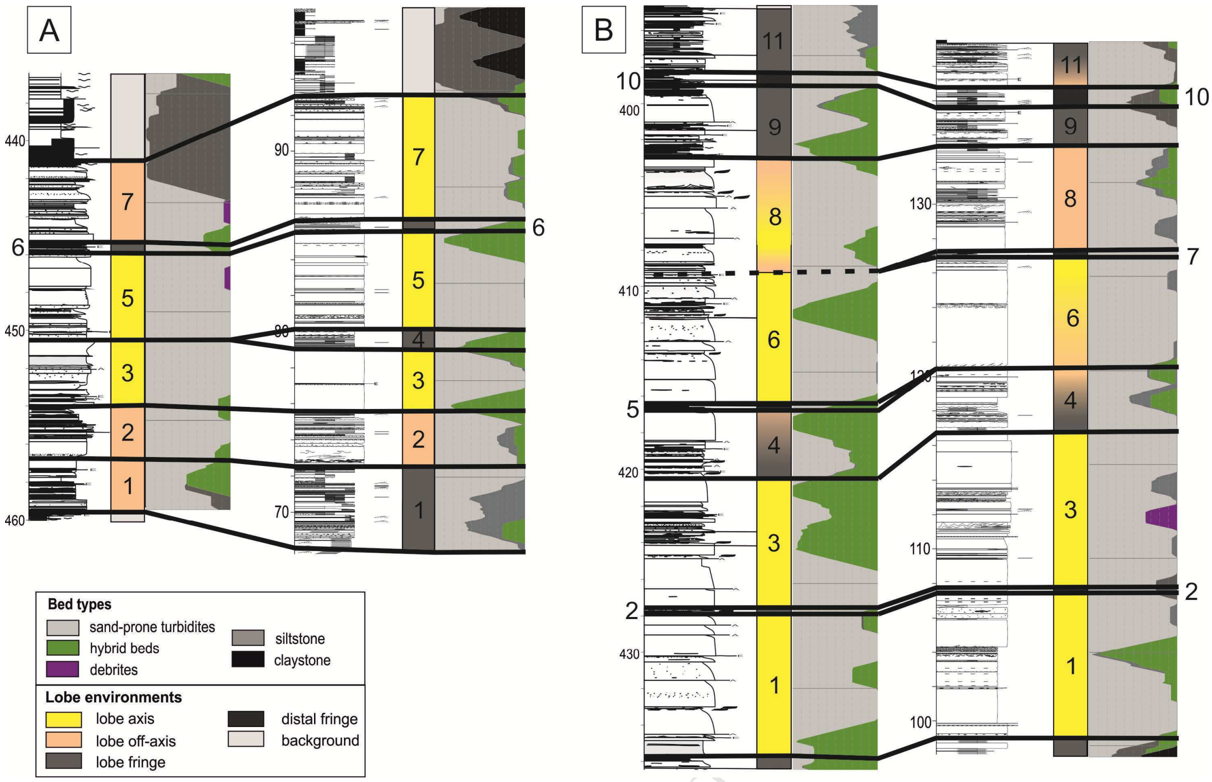
A
B
Bed types
sand-prone turbidites
hybrid beds
debrites
siltstone
claystone
Lobe environments
lobe axis
lobe off-axis
lobe fringe
distal fringe
background

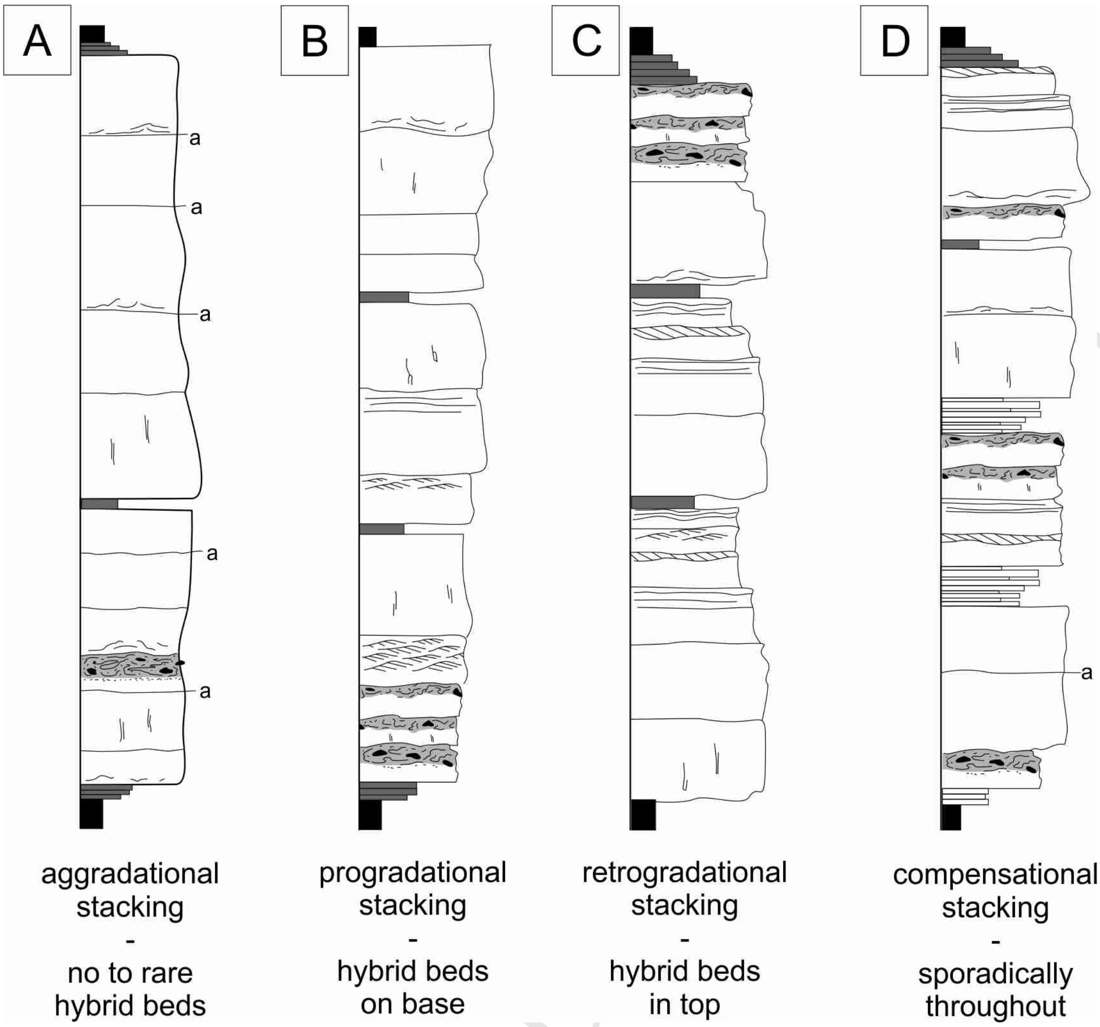
A
a
a
a
a
a
aggradational stacking
-
no to rare hybrid beds
B
progradational stacking
-
hybrid beds on base
C
retrogradational stacking
-
hybrid beds in top
D
a
compensational stacking
-
sporadically throughout

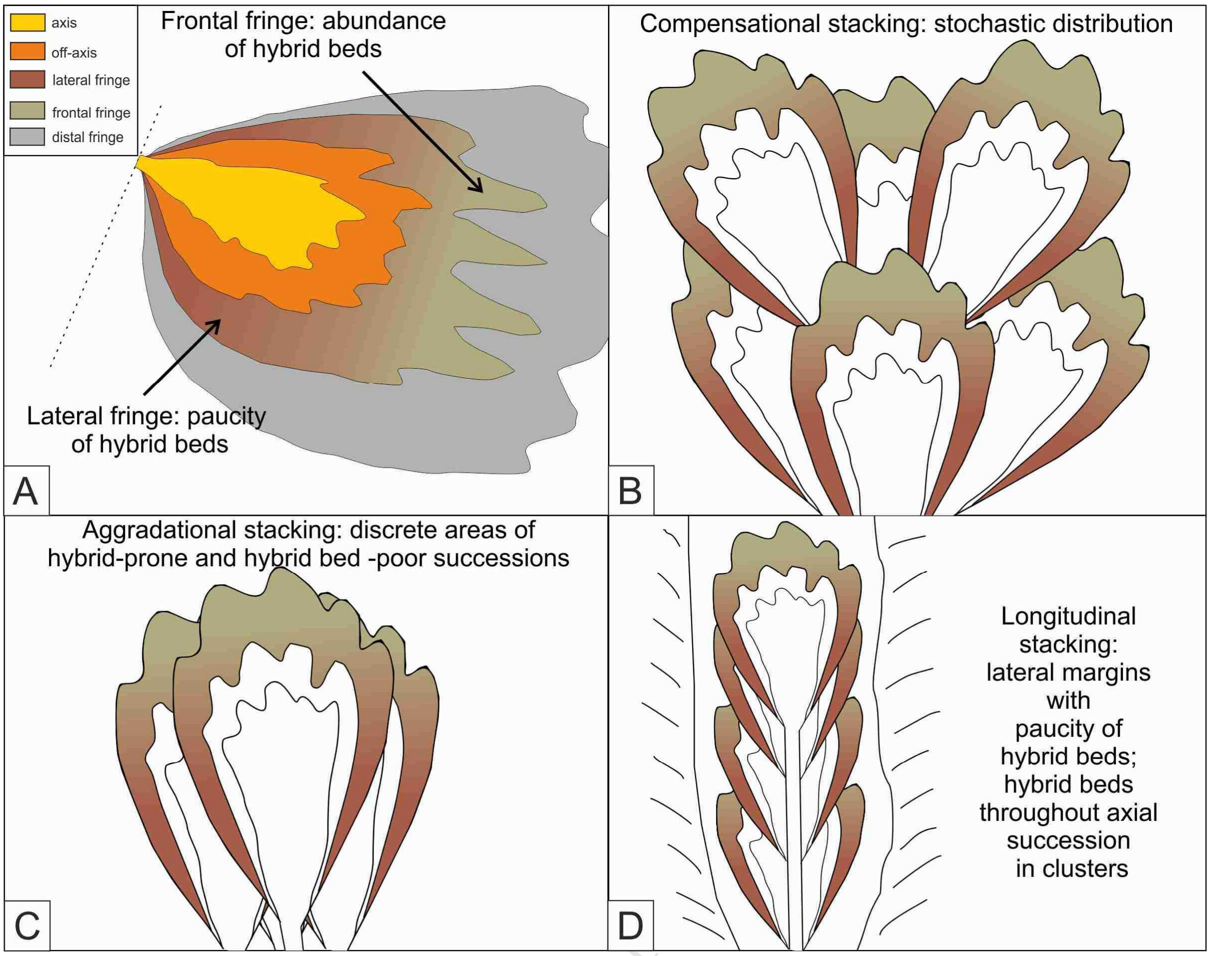
axis
off-axis
lateral fringe
frontal fringe
distal fringe
Frontal fringe: abundance of hybrid beds
Lateral fringe: paucity of hybrid beds
A
Compensational stacking: stochastic distribution
B
Aggradational stacking: discrete areas of hybrid-prone and hybrid bed -poor successions
C
Longitudinal stacking: lateral margins with paucity of hybrid beds; hybrid beds throughout axial succession in clusters
D

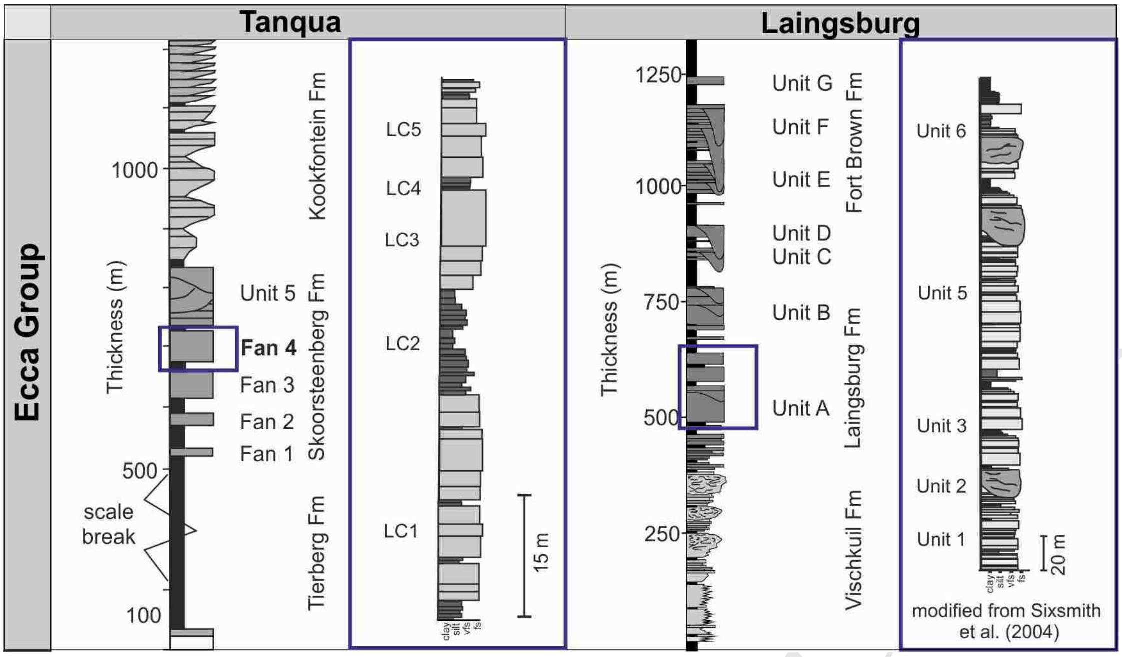

Tanqua
Laingsburg
Ecca Group
Thickness (m)
1000
500
100
scale break
Unit 5
Fan 4
Fan 3
Fan 2
Fan 1
Kookfontein Fm
Skoorsteenberg Fm
Tierberg Fm
LC5
LC4
LC3
LC2
LC1
15 m
clay silt vfs fs
1250
1000
750
500
250
Unit G
Unit F
Unit E
Unit D
Unit C
Unit B
Unit A
Fort Brown Fm
Laingsburg Fm
Vischkuil Fm
Unit 6
Unit 5
Unit 3
Unit 2
Unit 1
20 m
modified from Sixsmith et al. (2004)

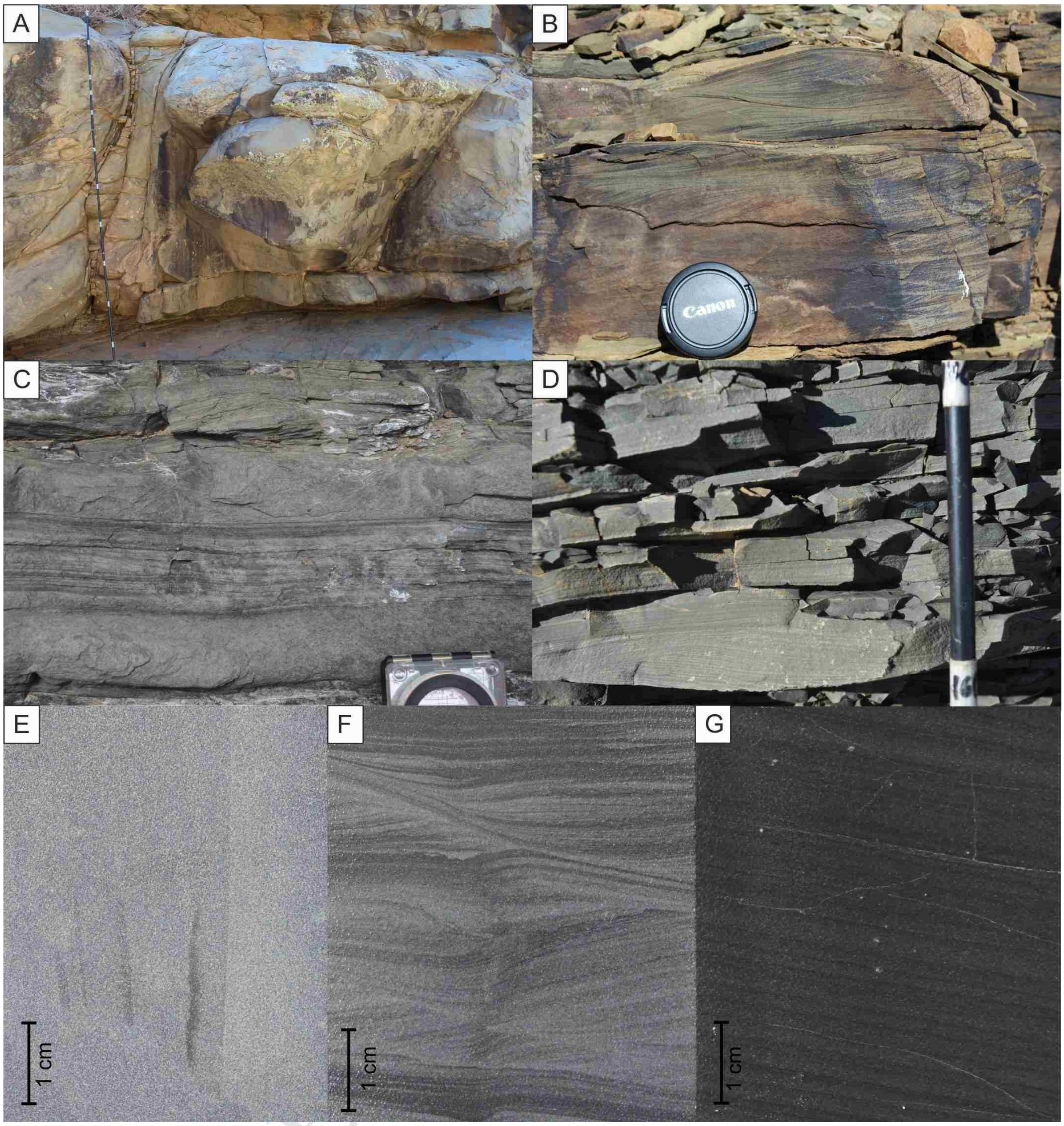
A
B
C
D
E
F
G
1 cm
1 cm
1 cm

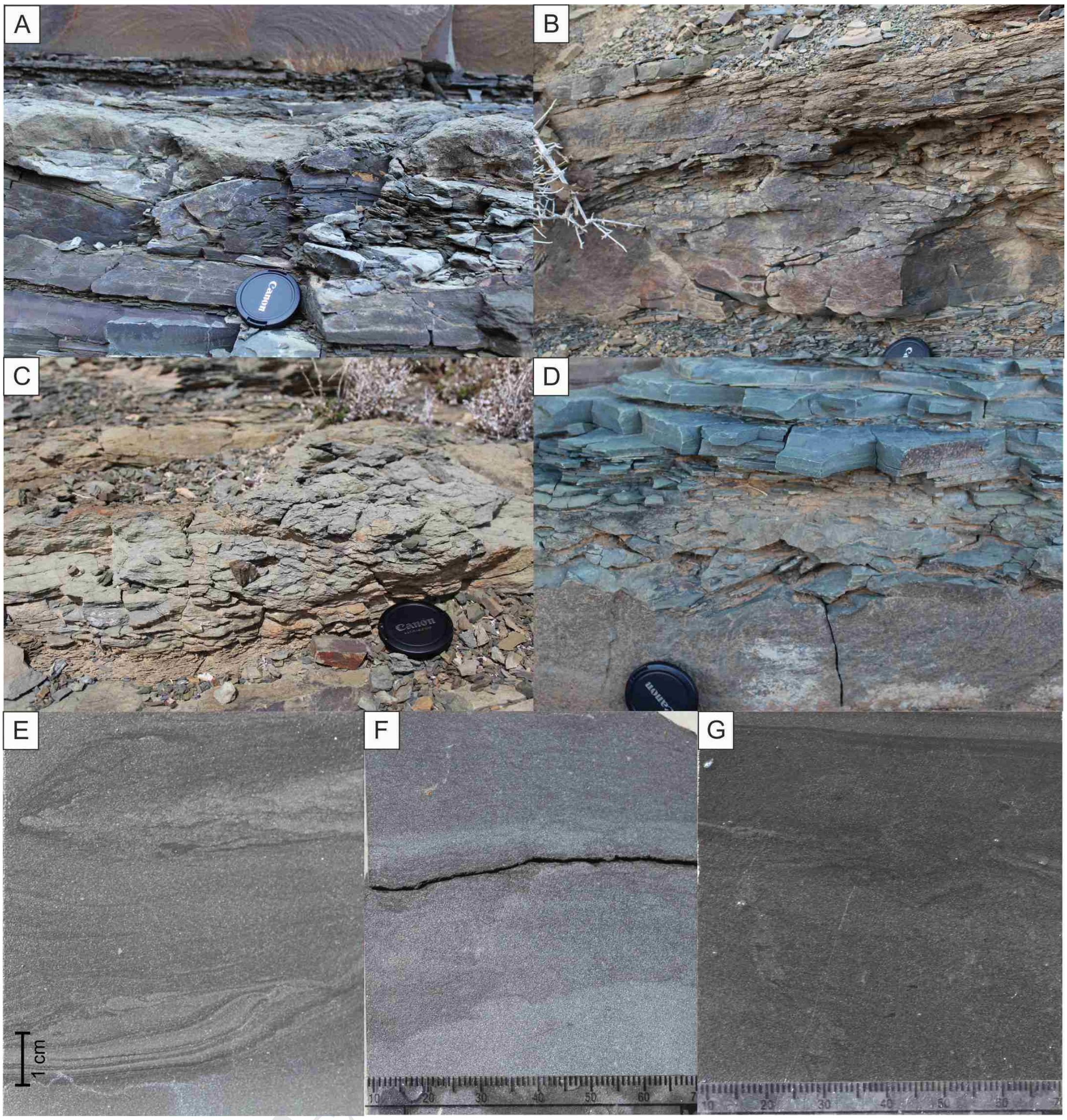
A
B
C
D
E
F
G
1 cm

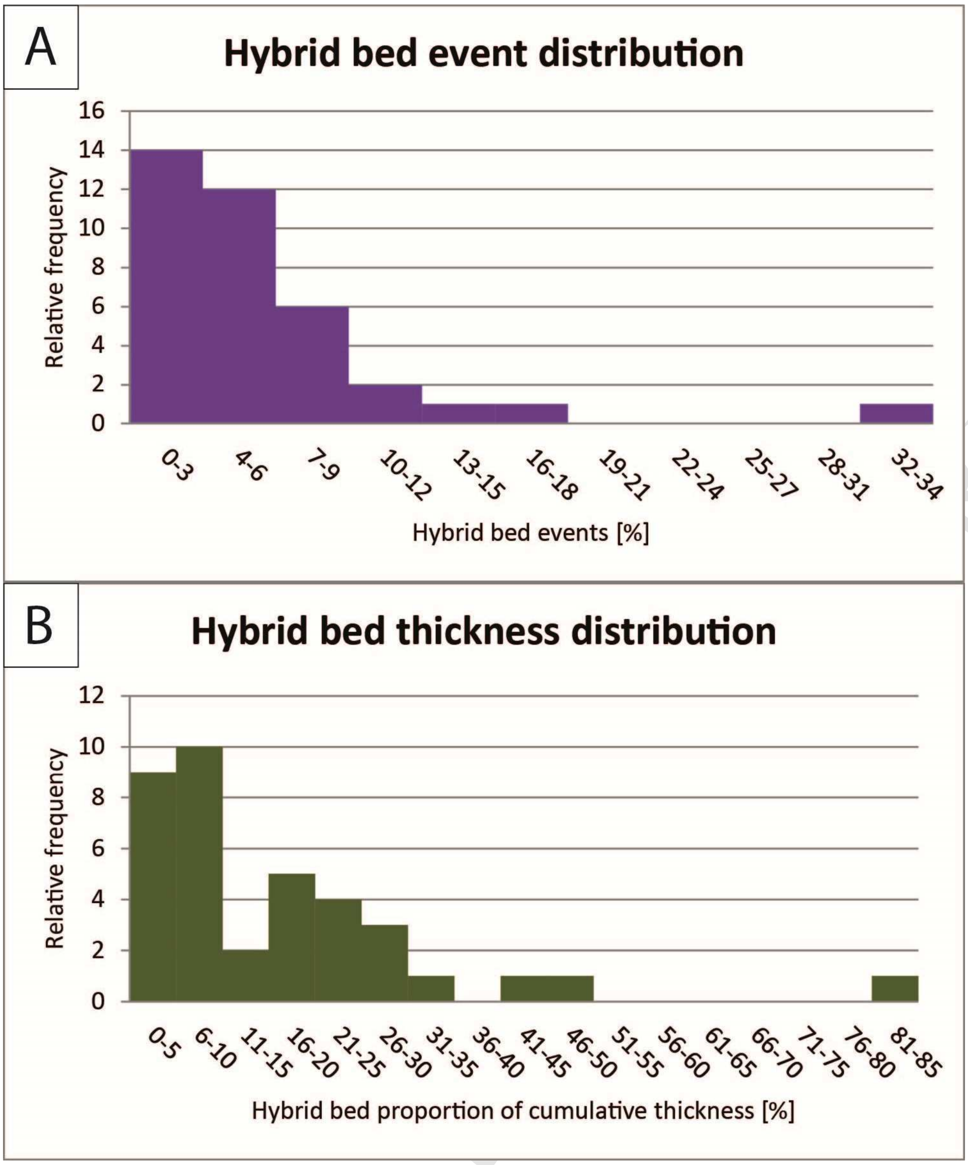
A
Hybrid bed event distribution
Relative frequency
16
14
12
10
8
6
4
2
0
0-3
4-6
7-9
10-12
13-15
16-18
19-21
22-24
25-27
28-31
32-34
Hybrid bed events [%]
B
Hybrid bed thickness distribution
Relative frequency
12
10
8
6
4
2
0
0-5
6-10
11-15
16-20
21-25
26-30
31-35
36-40
41-45
46-50
51-55
56-60
61-65
66-70
71-75
76-80
81-85
Hybrid bed proportion of cumulative thickness [%]

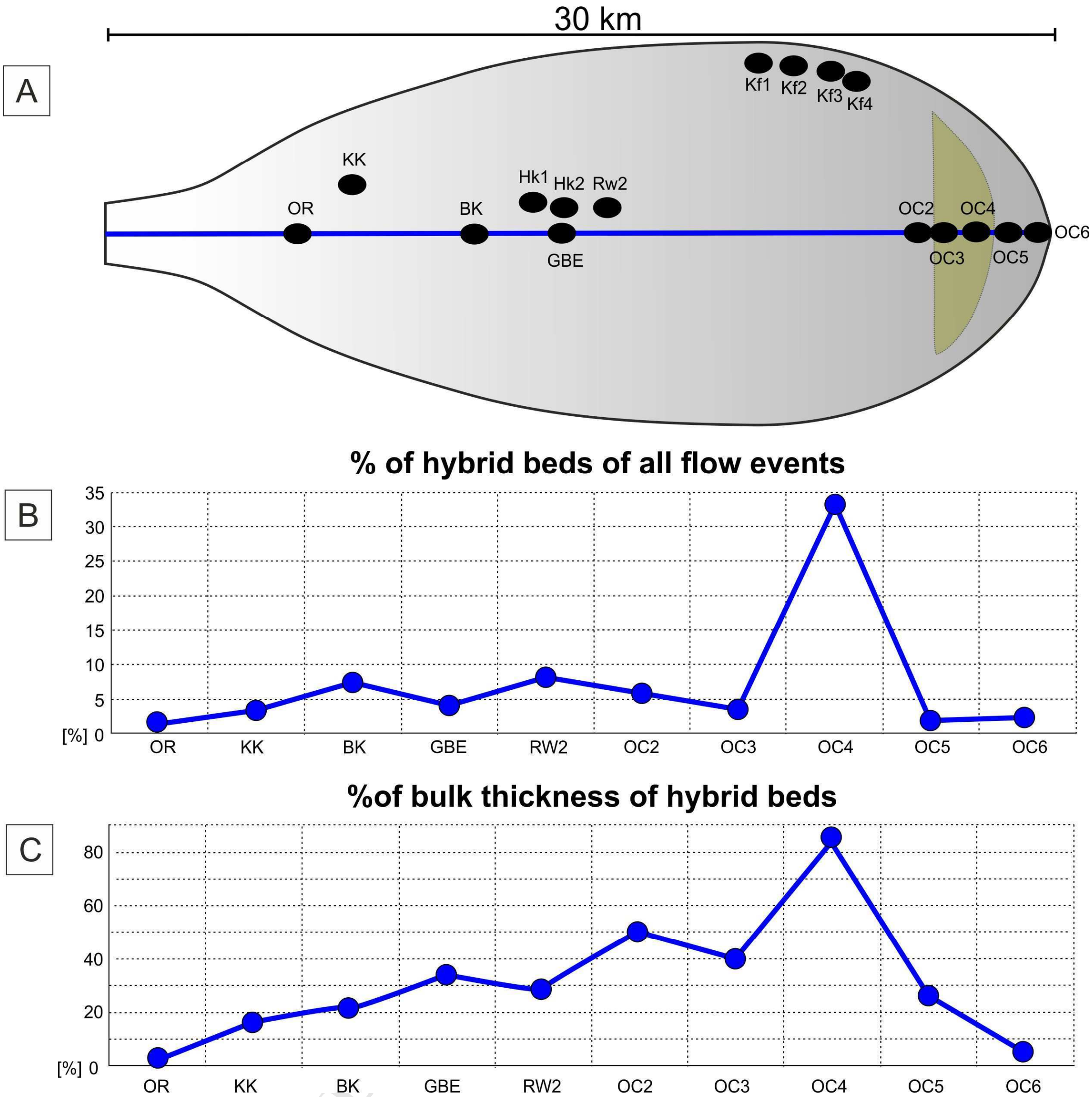
30 km
A
KK
OR
BK
Hk1
Hk2
Rw2
GBE
Kf1
Kf2
Kf3
Kf4
OC2
OC4
OC3
OC5
OC6
% of hybrid beds of all flow events
B
35
30
25
20
15
10
5
[%] 0
OR
KK
BK
GBE
RW2
OC2
OC3
OC4
OC5
OC6
%of bulk thickness of hybrid beds
C
80
60
40
20
[%] 0
OR
KK
BK
GBE
RW2
OC2
OC3
OC4
OC5
OC6

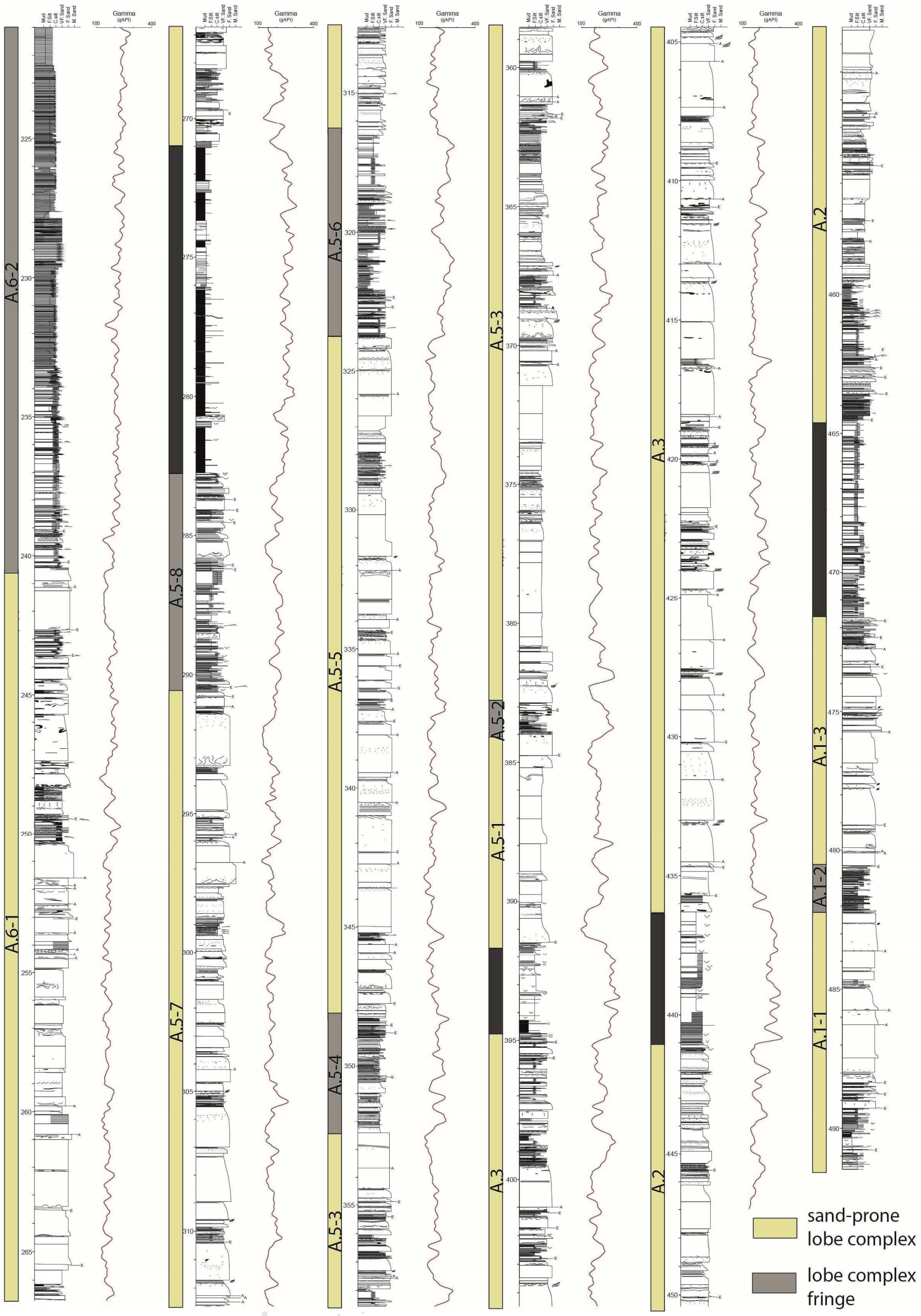
A.6-2
A.6-1
A.5-8
A.5-7
A.5-6
A.5-5
A.5-4
A.5-3
A.5-3
A.5-2
A.5-1
A.3
A.3
A.2
A.2
A.1-3
A.1-2
A.1-1
sand-prone lobe complex
lobe complex fringe

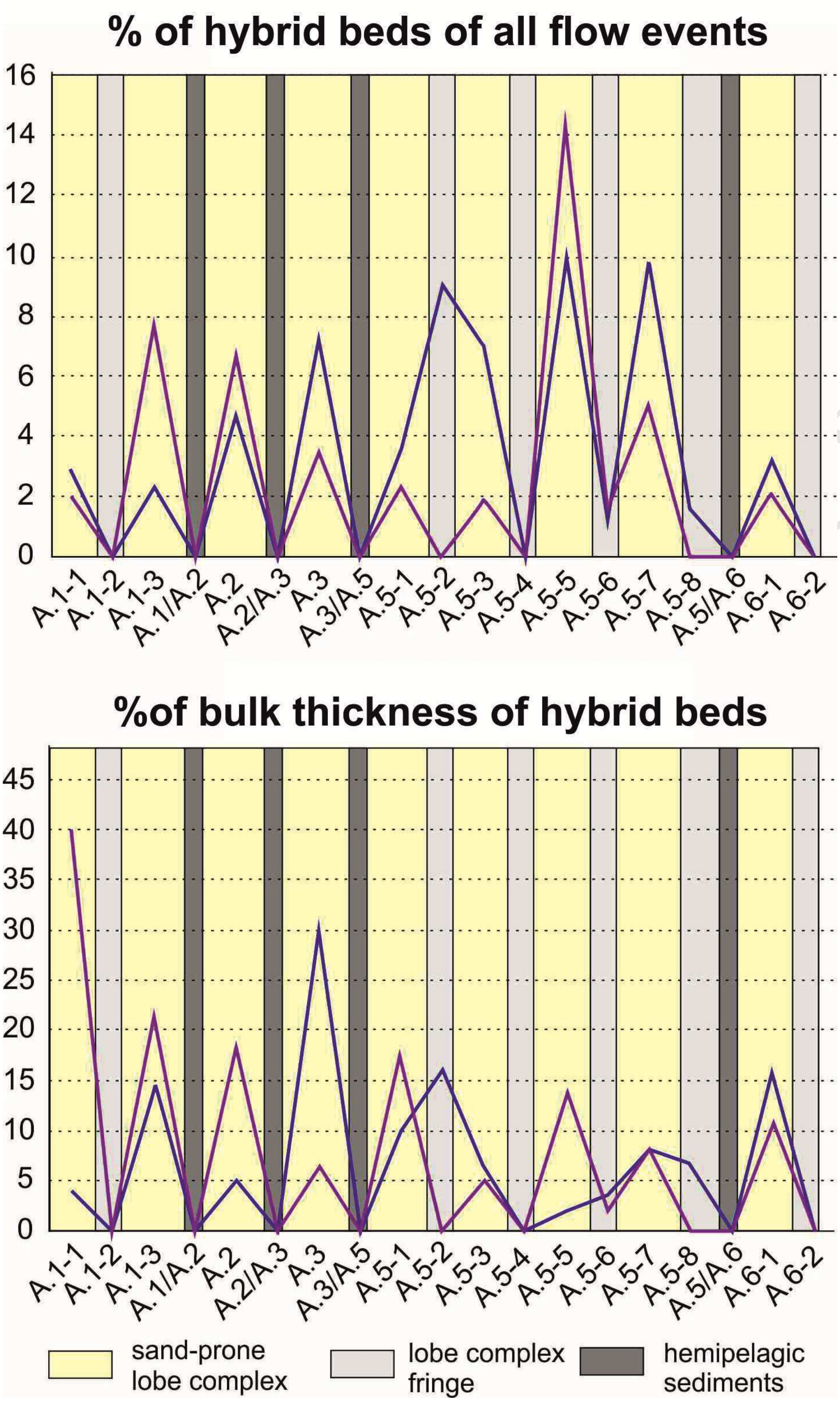

% of hybrid beds of all flow events
16
14
12
10
8
6
4
2
0
A.1-1
A.1-2
A.1-3
A.1/A.2
A.2
A.2/A.3
A.3
A.3/A.5
A.5-1
A.5-2
A.5-3
A.5-4
A.5-5
A.5-6
A.5-7
A.5-8
A.5/A.6
A.6-1
A.6-2
%of bulk thickness of hybrid beds
45
40
35
30
25
20
15
10
5
0
sand-prone lobe complex
lobe complex fringe
hemipelagic sediments

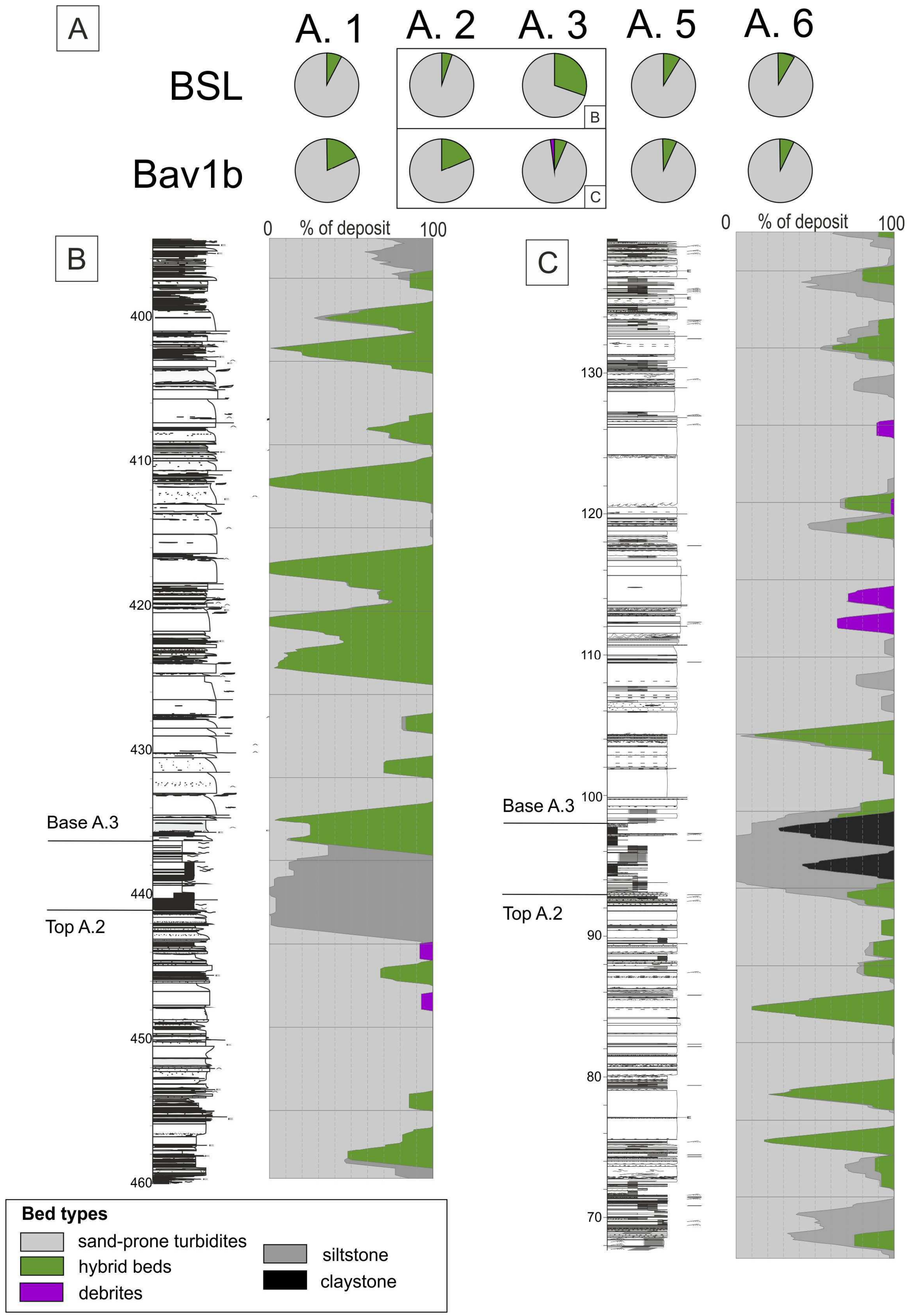

A
A. 1
A. 2
A. 3
A. 5
A. 6
BSL
Bav1b
B
C
0
% of deposit
100
400
410
420
430
440
450
460
Base A.3
Top A.2
130
120
110
100
90
80
70
Bed types
sand-prone turbidites
hybrid beds
debrites
siltstone
claystone

Highlights

- >23,000 individual beds have been evaluated for deposit type and bed thickness
- prominent geographical trend showing that hybrid bed deposits become more prevalent towards the frontal fringes of a lobe complex
- weak to no stratigraphic trend in the distribution of hybrid beds at the scale of a composite sequence set and lobe complexes
- distribution of hybrid beds is interpreted to be controlled by flow transformation processes on the basin-floor and dominant stacking pattern